

Review

Detailed Heat Transfer Measurements for Rotating Turbulent Flows in Gas Turbine Systems

Srinath V. Ekkad ^{1,*} and Prashant Singh ²

¹ Department of Mechanical & Aerospace Engineering, North Carolina State University, Raleigh, NC 27695, USA

² Department of Mechanical Engineering, Mississippi State University, Box 9552, Mississippi, MS 39762, USA; singh@me.msstate.edu

* Correspondence: sekkad@ncsu.edu

Abstract: Detailed understanding of hot gas path flow and heat transfer characteristics in gas turbine systems is imperative in order to design cooling strategies to meet the stringent requirements in terms of coolant usage to maintain critical components below a certain temperature. To this end, extensive research has been carried out over the past four decades on advanced thermal diagnostic methods to accurately measure heat transfer quantities such as Nusselt number and adiabatic film cooling effectiveness. The need to capture local heat transfer characteristics of these complex flow systems drives the development of measurement techniques and the experimental test facilities to support such measurements. This article provides a comprehensive overview of the state-of-the-art thermal diagnostic efforts pertaining to heat transfer measurements in rotating gas turbine blade internal and external cooling and rotor-stator disc cavity, all under rotating environments. The major investigation efforts have been identified for each of the above three categories and representative experimental results have been presented and discussed.

Keywords: gas turbines; rotating heat transfer



Citation: Ekkad, S.V.; Singh, P. Detailed Heat Transfer Measurements for Rotating Turbulent Flows in Gas Turbine Systems. *Energies* **2021**, *14*, 39. <https://dx.doi.org/10.3390/en14010039>

Received: 10 September 2020

Accepted: 24 November 2020

Published: 23 December 2020

Publisher's Note: MDPI stays neutral with regard to jurisdictional claims in published maps and institutional affiliations.



Copyright: © 2020 by the authors. Licensee MDPI, Basel, Switzerland. This article is an open access article distributed under the terms and conditions of the Creative Commons Attribution (CC BY) license (<https://creativecommons.org/licenses/by/4.0/>).

1. Introduction

There has been a continued push for higher turbine inlet temperatures as it directly affects the overall gas turbine efficiency. The resultant increase in the heat load on the components in the high-pressure stages in gas turbine engines is significant and well beyond the material capabilities to handle such harsh environments. To make this system possible, the turbine components are equipped with sophisticated cooling technologies, which are based on the relatively cooler air discharged from the compressor (~700 °C) bypassing the combustor. However, this discharge of pressurized air from the compressor also results in loss of overall gas turbine efficiency. Hence, it is imperative to strike a balance between the maximum coolant usage and the acceptable temperatures of the components exposed to hot combustor exit gases. In order to increase the turbine power output by 100%, the turbine inlet temperature needs to increase from 1700 °C to 2000 °C with the same amount of coolant usage, which is roughly 3–5% of the compressor discharge [1]. This increase in turbine inlet temperature will pose significant heat load and the constraint on the coolant usage makes the job of turbine cooling designers extremely challenging.

Figure 1 shows a typical complex flow network in the first few stages of turbine section. Hot gases from the combustor discharge first interact with the nozzle guide vanes and then the first stage of rotor. The red and blue arrows represent the high- and low-pressure air flow paths. The blue highlighted region is considered to be extremely critical as it directly encounters the hot gases exiting the combustor section and the rotating components further add to the thermal stresses, resulting in increased probability of component- or system-level failure. The rotating heat transfer research in this part of the gas turbine engine is primarily focused on the internal cooling of blades, rotor-stator disk cavity flow and heat

transfer, blade tip heat transfer and blade shroud heat transfer. The design of cooling technologies for the rotating components has its own unique challenges in the sense that the expected heat transfer correlations obtained under non-rotating conditions may not hold true under an engine-similar rotating environment. Furthermore, for efficient cooling concept development, it is important to accurately measure the heat transfer under the simulated rotating conditions. This review article is focused on the measurements under rotating conditions for the above-mentioned segments in the high-pressure turbine stages and they are discussed briefly here.

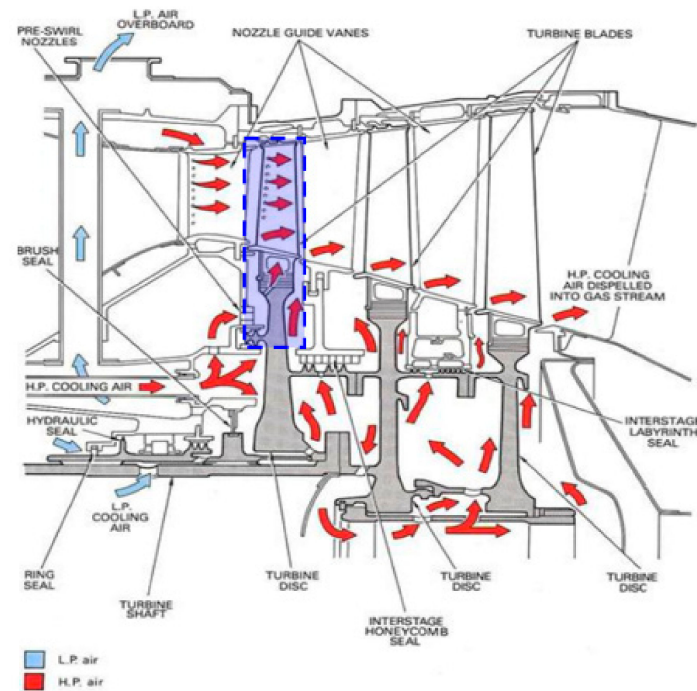


Figure 1. Flow paths in a high-pressure turbine stage [Source: The Jet Engine, 1986].

A typical blade from high-pressure turbine stage is shown in Figure 2. The blade from the outer side features a series of film-cooling holes that allow the coolant being routed in the internal passages to bleed and form a protective skin of relatively cooler fluid over the blade surface to reduce the effective heat flux from the hot gases flowing over the blades.

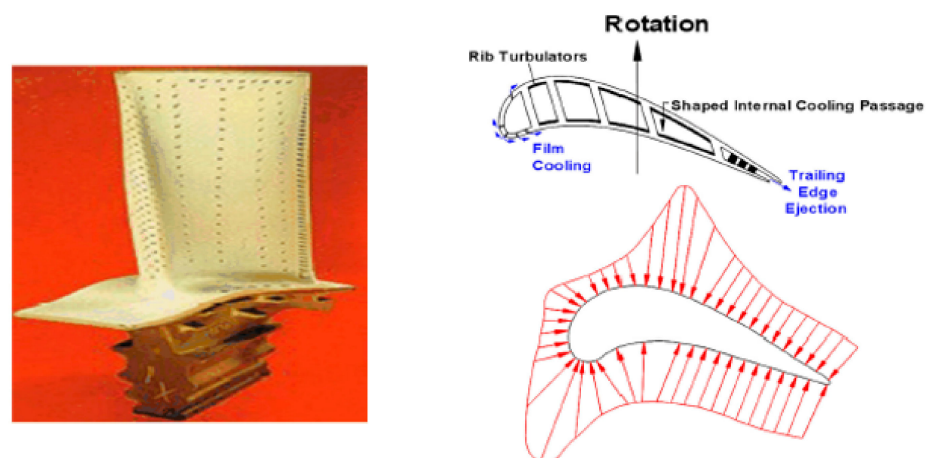


Figure 2. Blade film cooling holes, internal cooling cavities viewed from the top and representative heat load from hot gases on the blade outer skin [2].

The blade is essentially hollow with provisions for internal passages through which the coolant is routed to increase the heat transfer between the internal walls of the blade. Figure 2 also shows the cavities that feature turbulence promoters (rib turbulators), pin-fins etc. and the magnitude of the heat load in different regions of blade outer skin which dictates the internal and external cooling scheme. Much research has been carried out to quantify the convective heat transfer coefficient between the blade internal walls and the coolant for different segments in the gas turbine blade. For a comprehensive documentation on this topic, the reader is referred to [3].

The internal cooling scheme in gas turbine blades is typically comprised of serpentine passages in the mid-chord region, jet impingement through a row of circular jets in the leading-edge region and an array of pin-fins in the trailing edge (Figure 3).

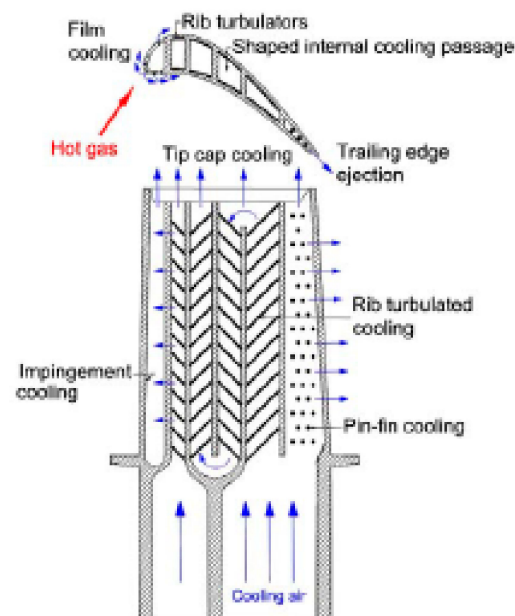


Figure 3. Internal cooling scheme in a typical gas turbine blade [2].

These cooling technologies are employed based on the cooling requirements, cooling space availability, etc. The cooling supply is typically divided into two streams where one line feeds the leading edge exclusively and the other feeds the mid-chord and the trailing edge regions. There has been extensive research on the internal cooling heat transfer both under stationary and rotating conditions, where several different designs of rib turbulators, pin-fin shapes and jet impingement hole shapes have been investigated with an aim to develop concepts that have high thermal hydraulic performance. This design criterion is considered important to meet the enhanced cooling capabilities with limited usage of the coolant air. In this article, the stationary condition heat transfer research is not included, and the reader may refer to [3] for details. The following sections in this paper will cover detailed heat transfer measurements for blade leading edge jet impingement, smooth and rib turbulator-featured mid-chord serpentine passages, dimpled passages and pin-fin heat transfer.

One other component of blade cooling is the tip and shroud, which is a challenging area as the extremely small clearance between the shroud and tip results in significant convective heat transfer loading due to hot gas high-speed flow. A typical turbine blade tip flow scenario is shown in Figure 4. There are very limited experimental investigations to capture the cooling characteristics of turbine blade tip and shroud due to inherent challenges associated with the rotating component and stationary temperature sensing device.

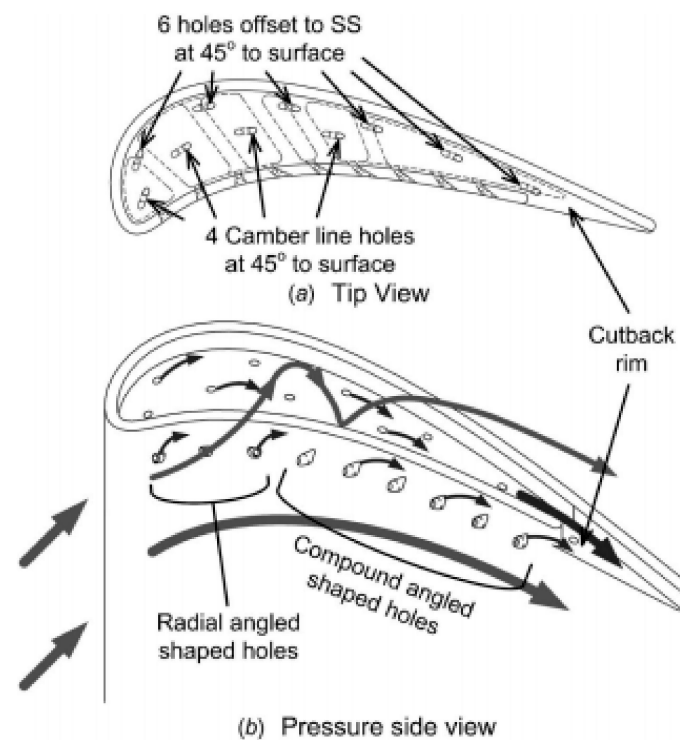


Figure 4. Turbine blade tip cooling [4]. Reprint with permission from ASME (order number 1084744).

The hot gases exiting the combustor section have a detrimental effect on the rotor-stator disk cavity, which are separated from each other by a fine clearance. The ingestion of these hot gases imposes cooling challenges in this section of the turbine. The cooling of rotor-stator cavity (Figure 5) is accomplished by bleeding the air extracted from the compressor discharge into the cavity through the stator hub (e.g., Figure 1). Extensive research has been carried out in this area to characterize the ingestion mechanism, the flow and heat transfer in the disc-cavity and the interaction of the coolant and the ingested hot gases, e.g., [5–7]. In this article, advanced thermal diagnostic techniques are presented that have been employed for measurement of convective heat transfer coefficients on the stator and rotor walls.

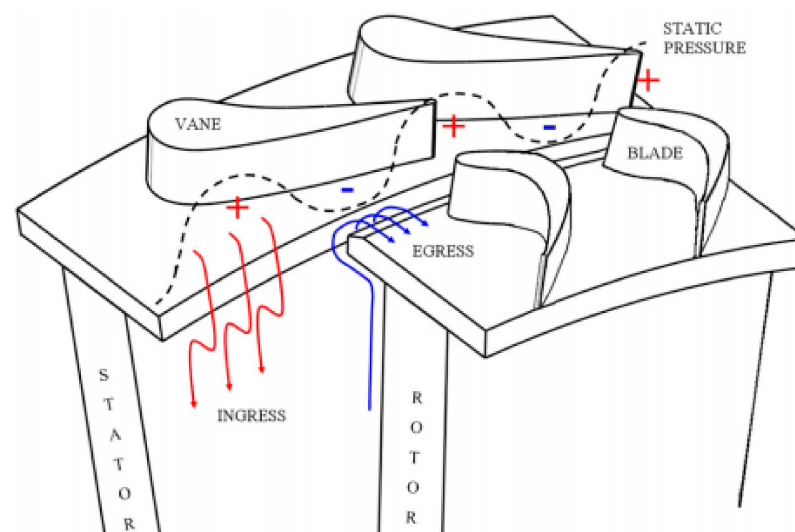


Figure 5. Rotor-stator disk cavity [5]. Reprint with permission from ASME (order number 1084750).

The above discussion emphasizes on the need for accurate and detailed measurement of heat transfer quantities to accurately predict the heat transfer loads in engine-similar conditions and to design suitable cooling technologies that can meet the gas turbine operational guidelines. This article is organized as follows: firstly, the experimental techniques are presented briefly, second, the experimental setup design and challenges involved in the rotating facilities are discussed, followed by important studies on the cooling segments mentioned above. The paper will conclude with a critical assessment of experimental techniques, experimental setups, and future trends in the rotating heat transfer measurements.

2. Heat Transfer Measurement Techniques

Various thermal diagnostic methods can provide detailed wall temperature measurements in these complex geometries. These temperatures can then be suitably used in heat diffusion governing equations in solids of interest to yield the heat transfer quantities such as wall heat flux, convective heat transfer coefficient and adiabatic film cooling effectiveness.

2.1. Liquid Crystal Thermography (LCT)

Liquid crystal thermography has now evolved into a robust technique over the years, which is very popular in turbine cooling community due to its ease of application on a surface and simple conversion to local wall temperature. Thermochromic liquid crystals in a micro-encapsulated form are sprayed on a surface, where these spherical particles ($\sim 20 \mu\text{m}$) are glued together via a suitable adhesive (also called “binders”). These *chiral nematic* structures when exposed to light of a suitable wavelength at a certain crystal temperature reflects light at a certain wavelength governed by Bragg’s reflection formula.

$$\lambda = npsin\theta \quad (1)$$

The reflected light from the surface is captured by a regular *Charged coupled device* (CCD) camera. The liquid crystal color change images captured by the CCD camera is interpreted in different ways through image processing tools to establish a relationship between an incident in color change process to a surface temperature. More details on liquid crystal thermography can be found in Ireland and Jones [8] and its applications in [9]. Different methods for color change to wall temperature conversion are presented in Camci et al. [10] and Hay and Hollingsworth [11].

Calibration Methods in Liquid Crystal Thermography

There are many methods of calibrating liquid crystal color change with local wall temperature. For calibration, a repeatable event is required which can be related to local instantaneous wall temperature. The calibration methods rely on surface thermocouples. The LCs can be calibrated in many different ways:

- a. A steady temperature gradient can be maintained on the surface coated with LC, and with known temperature values on the two ends, a linear curve can be drawn and equated to local color content.
- b. Surface coated with LC can be maintained at a fixed temperature and the LC image is recorded at small temperature increments to obtain the complete color play band.
- c. There are transient methods as well for LC calibration and is mostly adopted for in-situ calibration. A wall thermocouple is typically mounted on the surface in the vicinity of the region of interest very convective heat transfer coefficient is to be calculated. The fluid assisted heating or cooling drives the change in the surface temperature, and with the help of a CCD camera, the entire color change can be recorded and later processed in conjunction with the local wall temperature measurements.

Method (c) above is very popular in forced convection type studies where in-situ calibration is preferred to ensure that the lighting conditions were same during the calibration

and in the actual forced convection experiment. However, experimental setups can be designed where methods (a) or (b) can be used in forced convection type experiments, where exact same lighting conditions can be maintained, just the calibration will not be in-situ in that case. Above methods present different ways in which color-temperature relationship can be established. There are many methods to process the color change also. For example, one can track an incidence such as start of red or green color, or find the instance where peak red or peak green color occurred during the heating or cooling process and related these occurrences to the measured local wall temperature. The idea behind such practices is to locate an incidence which corresponds to an exclusive wall temperature, which reduces the errors in calibration. A different method is to convert red, green and blue color contents to Hue, Saturation and Intensity values. Through many prior studies, a near linear or 2nd or 3rd order polynomial relationship has been observed between Hue and wall temperature. This method has been proven to be more robust as it offers a unique Hue-temperature pair, and multiple of such pairs can be obtained through a simple calibration run through any of the three methods mentioned above (Figure 6). Camci et al. [10] have reported extensive investigation on HSI method of calibration and showed that it is less sensitive towards the ambient conditions. A sample HSI calibration curve is shown below.

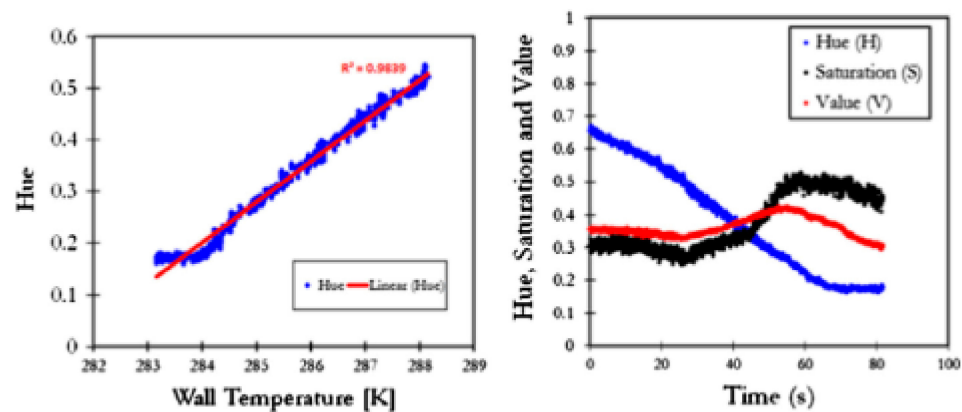


Figure 6. Hue, saturation, intensity calibration from Singh and Ekkad [12]. Reprint with permission from Elsevier (order number 4961560858625).

2.2. Infrared Thermography (IRT)

Infrared thermography involves conversion of energy radiated by an object to the infrared band of the electromagnetic spectrum, a technique which is eventually converted to electronic signals. These signals are then processed for display as an image e.g., in grey scale mode or a color mode where the intensity or color respectively, correspond to a temperature. In short, IRT can be considered as a temperature measurement device. More details on IRT and its application can be found in ([13], Chapter 6). The calibration of the temperature output from the IR camera is also important since it requires the input of surface emissivity. Above calibration can be achieved in two different ways: (1) by measuring surface temperature via thermocouple and finding emissivity post the calibration run through establishing linear relationship between IR temperature output and thermocouple output. The entire surface temperature time history can then be mapped based on the above established relationship. (2) finding surface emissivity through above method and enter that as an input to the software managing the IR output, such that accurate temperature is output directly from the software and any post-processing of the time-temperature history is not required. Note that IR calibration is also very sensitive to the distance between the sensor and the surface and an angle between the surface and the IR camera sensor. A sample calibration procedure and curve are shown below in Figure 7 [13].

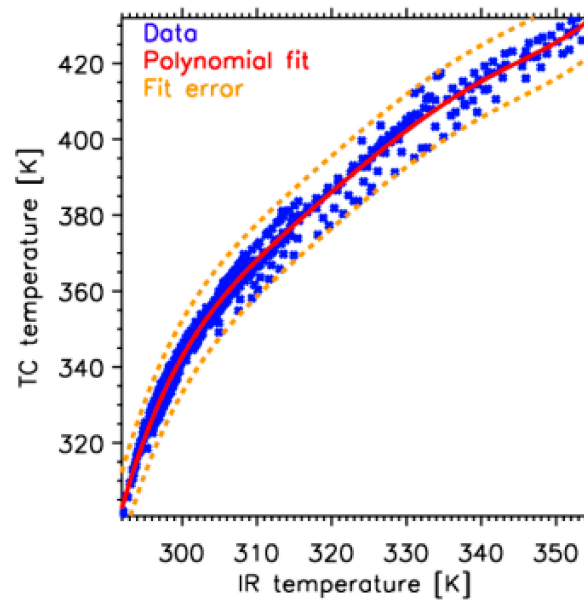


Figure 7. Infrared thermography calibration based on wall mounted thermocouples [13].

2.3. Transient Techniques Using One-Dimensional Semi-Infinite Conduction Modeling

One technique based on thermochromic liquid crystals (TLC) is where a solid can be treated as semi-infinite during short duration transient experiments. These solids are typically made of clear acrylic with thermal conductivity (k_s) of ~ 0.2 W/mK and thermal diffusivity (α) of $\sim 1.1 \times 10^{-7}$ m²/s. The wall temperature (T_w) evolution with time for a solid initially at T_i subjected to sudden change in ambient fluid temperature (T_m) is given as,

$$T_w(t) = T_i + (T_m - T_i) \left(1 - \exp\left(\beta^2\right) \operatorname{erfc}(\beta) \right) \quad (2)$$

where $\beta = h\sqrt{\alpha t}/k$. With the knowledge of one time-temperature pair (t, T_w), heat transfer coefficient h can be found in detailed measurements any error minimization routine. More details about this method through studies conducted by the authors can be found in [13] and the application of this technique to other scenarios can be found in [14–17].

2.4. Steady-State Experiments on Metallic Surfaces

Convective heat transfer coefficients can also be determined through steady state heat transfer experiments where a known surface heat flux is applied on the solid and the local wall temperature at the steady state is measured using liquid crystals or IR camera for detailed measurements, as shown in figure and the fluid temperature is measured by a wall thermocouple. The convective heat transfer can be written as,

$$h = \frac{q''}{T_w - T_f} \quad (3)$$

The employment of above techniques will be discussed again for specific experiments under different rotation scenarios.

2.5. Heat/Mass Transfer: Naphthalene Sublimation

The naphthalene sublimation technique is based on heat-mass transfer analogy and considered to be one of the most effective methods for local heat transfer coefficient determination, particularly in the situations with large thermal gradients where above mentioned techniques may yield in significant errors due to lateral conduction. Goldstein and Cho [18] have provided a comprehensive analysis of this method.

2.6. Adiabatic Film Cooling Measurements Using Pressure Sensitive Paints (PSP)

As shown in Figure 2, the gas turbine blade is externally cooled as well through bleeding of blade internal cooling air through an array of film holes. This creates a cooler protective film on the blade outer skin that essentially reduces the net heat flux into the blade from the hot gases. There have been many investigations on the quantification of adiabatic film cooling effectiveness by different experimental techniques based on thermocouple, TLC and IR thermography. A detailed account of that can be found in [3]. Post 2005, there have been a surge in the film cooling studies based on pressure sensitive paints (PSP), a technique originally proposed by Zhang and Fox in 1999 [19]. This technique to determine the film cooling effectiveness is based on oxygen quenching and does not have the issues of lateral heat diffusion on the surface, target surface material, relative temperature difference between mainstream temperature and the target surface temperature. A detailed account of the working principle of this technique and its application in many different turbine cooling segments is provided by Han and Rallabandi [20].

Wright et al. [21] have reported a detailed comparison between the three different techniques to measure adiabatic film cooling effectiveness, viz. PSP, TSP, IR, where TSP stands for Temperature Sensitive Paints.

3. Experimental Facilities for Rotating Heat Transfer Measurements

3.1. Turbine Blade Internal Cooling Research Facilities

Although the research on turbine blade internal cooling under rotating conditions dates to the late 1980s and early 1990s, the experimental facilities were steady-state copper heater based which provided region-wise averaged heat transfer coefficient. For example, an experimental program at The Gas Turbine Laboratory, Massachusetts Institute of Technology (MIT) on impingement heat transfer was the first, focused on rotating heat transfer [22]. The same group at MIT later carried out a series of experimental investigations on rotor blade heat transfer [23], film-cooling [24], etc. Some other noteworthy experimental programs are the rotational heat transfer investigations on multi-passage rib roughened and smooth channel at United Technologies Research Center (UTRC) in East Hartford, CT, USA, by Johnson and team [25–28]. The Turbine Heat Transfer Laboratory at Texas A&M University (TAMU) directed by Han, J.-C. housed a rotating heat transfer facility for turbine blade internal cooling measurements for two-passage rib roughened ducts, single-passage ducts with different aspect ratios, leading edge jet impingement, etc. [29–31]. The TAMU group since then has published over 200 archival publications on the topic of rotating heat transfer for roughened ducts. There have been some other groups as well who have contributed immensely towards rotating heat transfer field in the 1990s and have not be described here in the interest of brevity, e.g., [32–34].

Following discussion includes selected studies on detailed heat transfer coefficient and film cooling effectiveness under rotating conditions, where the experimental facilities and representative datasets obtained are introduced to the reader. We have tried to present these studies in a chronological order. The topic-specific sections on different segments in rotating components will provide a detailed account on the data.

The above-mentioned rotating heat transfer studies [22–34] are considered benchmark in the field and widely cited for both experimental and numerical validation. With the advancements in the detailed surface temperature measurements, there has been a constant push to resolve local heat transfer characteristics since the value of those datasets results in filling up the knowledge gap, which region-wise averaged heat transfer data cannot provide. To this end, some of the existing detailed heat transfer coefficient measurement techniques, such as a popular mass transfer technique based on heat and mass transfer analogy was extended to rotating systems, using Naphthalene sublimation technique. This technique is essentially based on post-processing where in-situ measurements under rotating conditions were not required –, and this proved to be a major advantage compared to thermal diagnostic methods at that time.

3.1.1. Turbine Blade Internal Cooling: Mass Transfer Methods

Lau et al., at Texas A&M [35] led the efforts on mass transfer experiments under rotating conditions and presented detailed heat transfer coefficient for leading, trailing and blade tip underside. Figure 8 shows the test rig that was used to carry out these measurements. The local Sherwood number ratio (Sh/Sh_0) contours have been shown in Figure 9 for both smooth channels under rotating and stationary conditions. The valuable information on the local heat transfer characteristics revealed fine details in the sharp-bend region and the differences between leading and trailing sides for radially inward and outward flows.

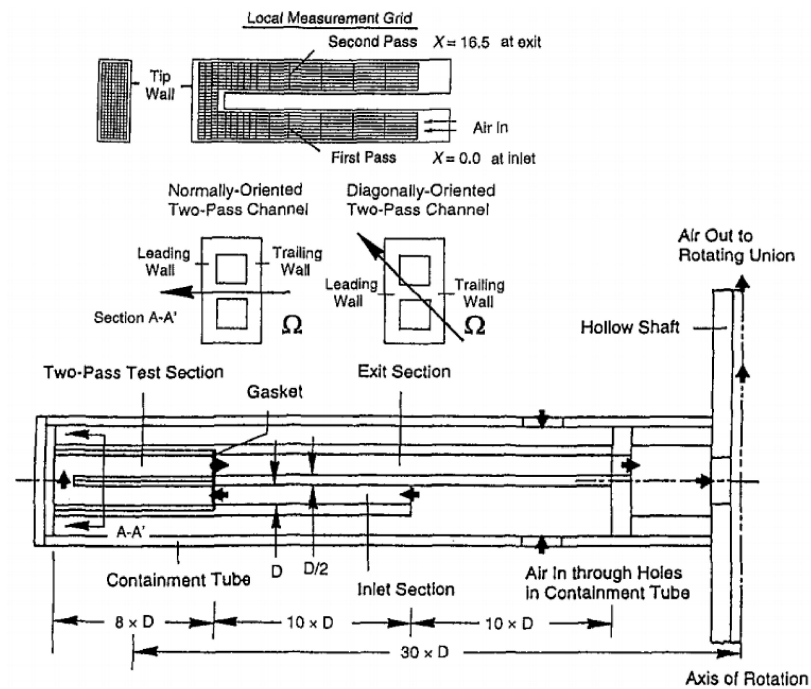


Figure 8. Mass transfer experiments under rotating conditions [35]. Reprint with permission from ASME (order number 1084745).

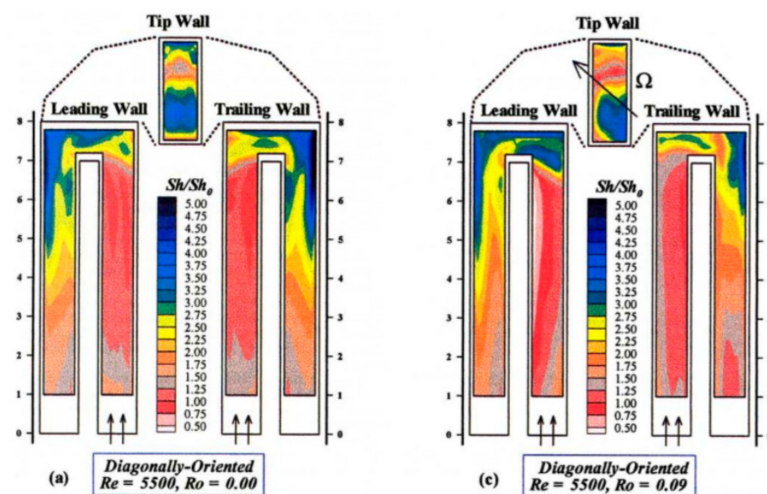


Figure 9. Local Sherwood Number (Sh) ratio (Sh/Sh_0) under stationary (left) and rotating conditions (right) [35] Reprint with permission from ASME (order number 1084745).

3.1.2. Turbine blade internal cooling: Infrared Thermography

Chang et al. [36] were one of the first to employ infrared thermography technique under steady-state heat transfer condition to measure the surface temperature under rotating condition for wide range of Rotation numbers and Buoyancy parameters. This method had its own advantage such as different wall temperatures maintained to achieve high density ratios ($\Delta\rho/\rho$), and their test facility shown in Figure 10a had provisions to accommodate large test sections that lateral heat diffusion enabled high Rotation number ($\omega D/V_c$) at relatively moderate rotational speeds. Further, Infrared thermography provides advantage over liquid crystal thermography as it provides local wall temperature in the entire operation range as opposed to only a fixed narrow band thermochromic liquid crystal. One limitation in this experimental method is the effect of lateral heat diffusion, which is stronger in the case of metals. Although gas turbine blade walls are made with metal alloys, the aim behind the convective heat transfer experiments is to capture the contribution of the fluid domain and testing conditions, which includes Reynolds number, Rotation number, Buoyancy parameter, etc. The added effect of metal - assisted heat diffusion skews the heat transfer results and, hence, should be used with caution.

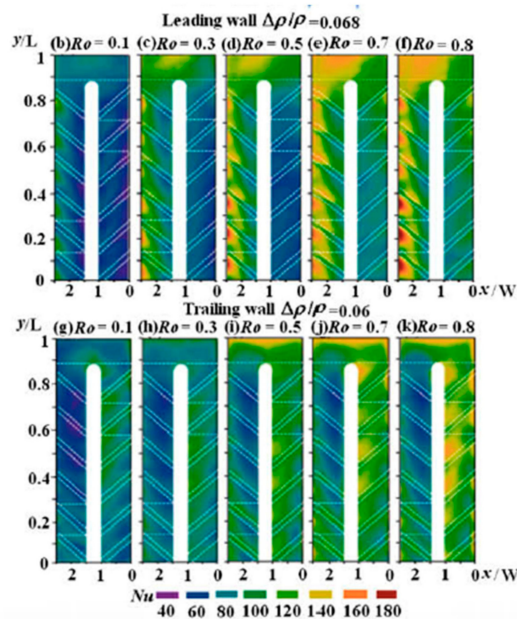
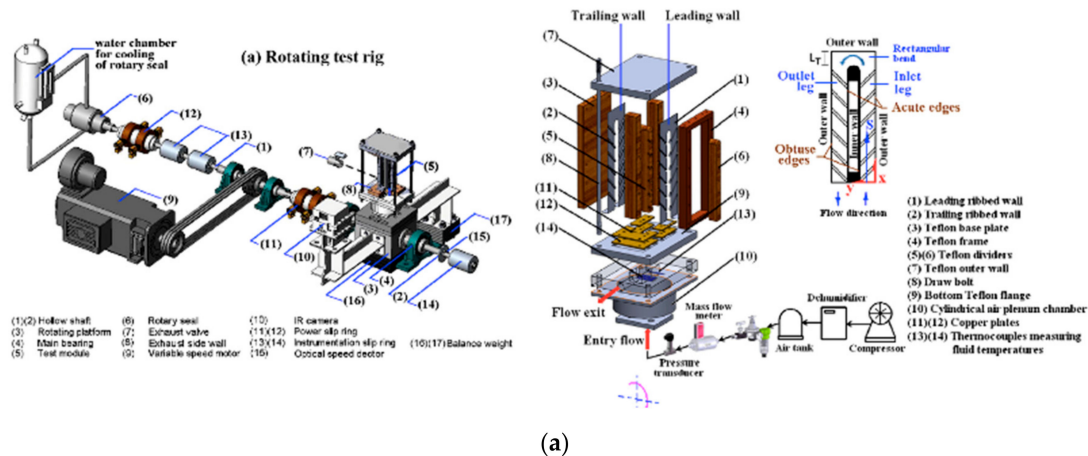


Figure 10. (a) Rotating rig facility employing Infrared thermography by Chang et al. [36], (b) detailed Nusselt number ratio (Nu/Nu_0) ratio under rotating conditions (Ro varied from 0.1 to 0.8) Reprint with permission from Elsevier (order number 4955590102249).

This study by Chang et al. [36] and many more (to be discussed later) can be considered a *gamechanger* in the rotating heat transfer measurements, as (1) detailed local heat transfer measurements could be obtained, (2) high Rotation numbers (engine-similar) could be obtained with the experimental facility, and (3) the aiding and opposing roles of Buoyancy in the serpentine passages could be studied since the facility allowed wide range of density ratios. The results hence generated had the best of both- highly controlled testing conditions obtained in steady-state heat transfer experiment (which yielded in region-wise averaged Nu ratio, e.g., [22–33]) and local heat transfer coefficients (Figure 10b), which typically employed transient heat transfer experiments (in which such control over testing conditions is limited at best) which will be discussed later in this sub-section.

3.1.3. Turbine Blade Internal Cooling Heat Transfer: Transient Liquid Crystal Thermography

Transient liquid crystal thermography (*TLCT*) experiments are popular in the gas turbine heat transfer community due to its simplicity in application in complex internal and external cooling scenarios, robust calibration, repeatable and detailed heat transfer coefficient and adiabatic film cooling effectiveness results. More details on this technique can be found in Ekkad and Han [9]. Although Blair et al. [37] were technically the first ones to have successfully used liquid crystals under rotating conditions, the dataset generated was of limited quality due to then limitations of available equipment. The group at Northeastern University led by Taslim [38] have also demonstrate the use of liquid crystals in their rotating rig facility for smooth and ribbed radial channels using steady-state experimental technique. In the interest of brevity, we have dropped these studies from discussion, to focus more on detailed heat transfer maps. To the best of authors' knowledge, Lamont et al. [39] were the first to use the *TLCT* using one-dimensional semi-infinite conduction modeling in rotating conditions to measure detailed convective heat transfer coefficients in two-passage ribbed channels.

The experimental test facility is shown in Figure 11a,b. This test rig [40] can accommodate complex internal cooling passages such as rib turbulators [41] and jet impingement [42]. In this experimental test rig, the liquid crystal color change was capture by a CCD camera mounted on the test section itself. The camera was also rotated with the test section through the transient test. These experiments used relatively colder air to get the buoyancy force direction right, and with a liquid crystal color play band between 10 and 15 °C, a hue-based method was adopted to find the time taken by a certain pixel to reach a reference solid temperature that lies in the color play band, and with that information, the local convective heat transfer coefficient was determined.

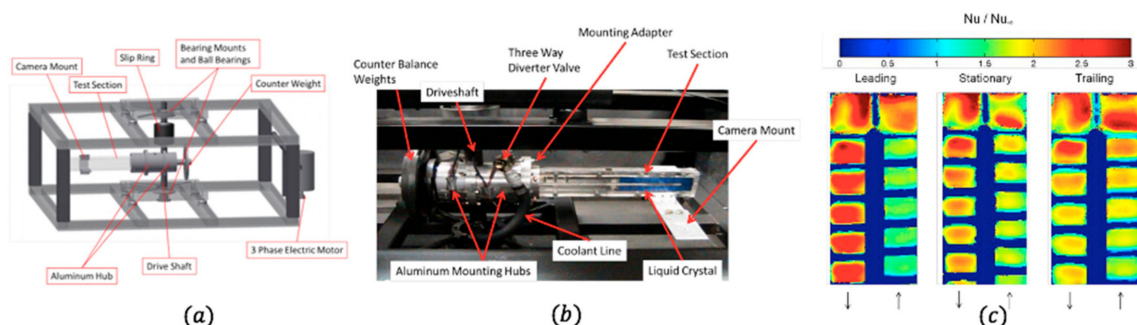


Figure 11. (a) Rotating heat transfer facility [40], (b) test section, (c) detailed Nusselt number ratio (Nu/Nu_0) [40].

The facility also allows in-situ calibration of the liquid crystals in each experimental run. This experimental method has been proven to be very efficient in obtaining detailed heat transfer coefficient in quick turnaround time, with high degree of repeatability. The limitations of this test rig include the low Buoyancy numbers due to the limitations imposed by the liquid crystal color change band. Further, due to the transient nature of experiments, the fluid temperature would drop continuously throughout the experiments,

which rendered the density ratio, buoyancy number time-variant. The engine-similar conditions on Rotation numbers and Buoyancy numbers were tough to achieve due to above-mentioned constraints imposed by the nature of experiments. More datasets obtained using this test facility on several different cooling concepts of gas turbine blade is discussed at a later stage.

There are several other facilities (Figure 12) that have been commissioned in past five years or so, e.g., the rotating rigs at the University of Florence, Italy [43], the Ohio State University, USA [44], the University of Stuttgart, Germany [45], National Chiao-Tung University, Taiwan [46], and von Karmann Institute, Belgium [47], to name a few. Figure 10 showcases the experimental facilities at the academic institutes mentioned above.

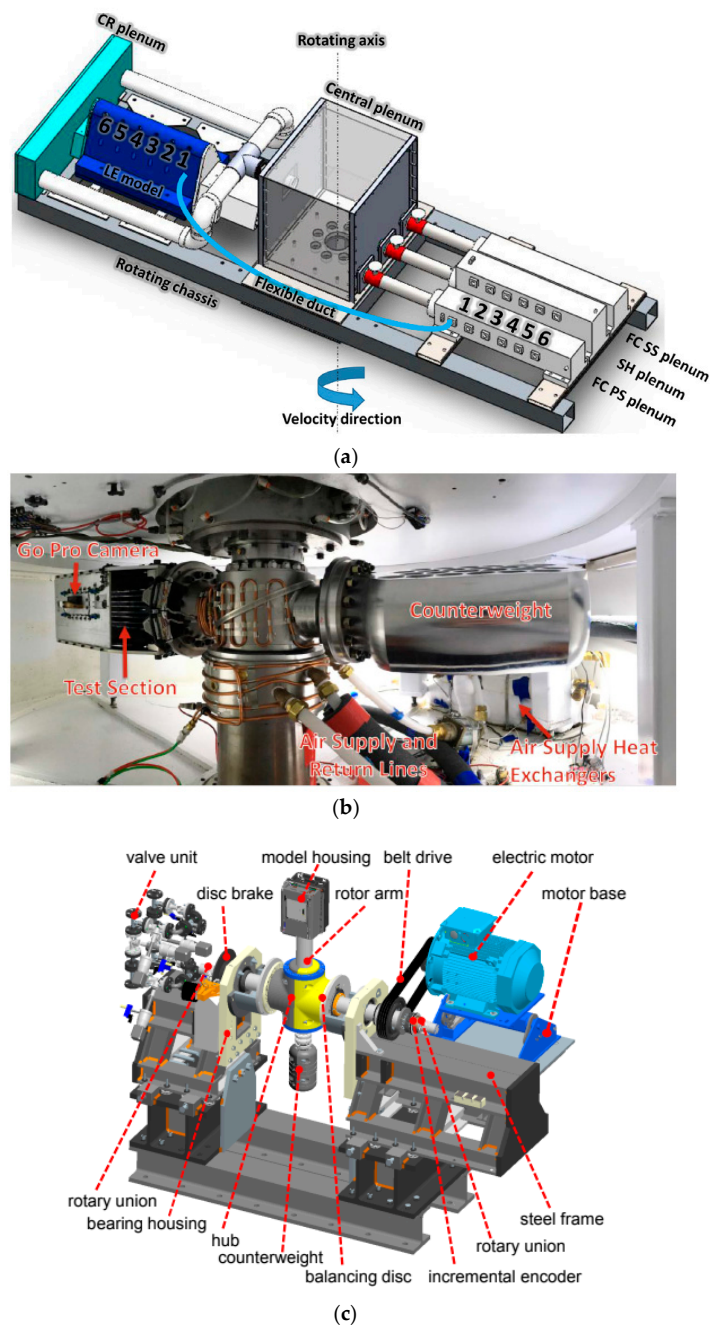


Figure 12. Cont.

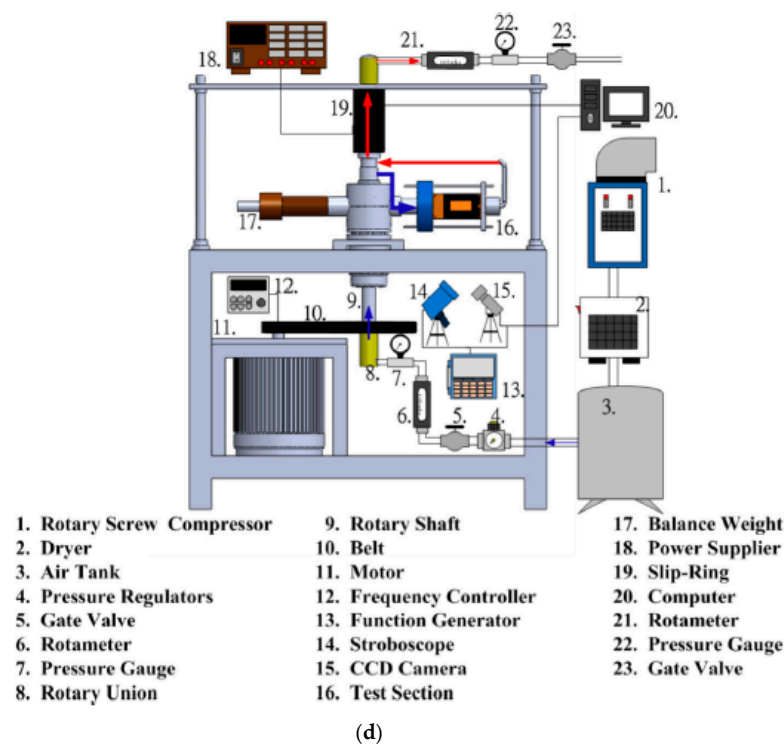


Figure 12. Rotating heat transfer test rigs at, (a) University of Florence, Italy [43], Reprint with permission from ASME (order number 1084747), (b) Ohio State University, USA [44] (c) University of Stuttgart, Germany [45], (d) National Chiao-Tung University, Taiwan [46].

3.2. Film Cooling Effectiveness Measurement (under Rotation) Facilities

The measurement of adiabatic film cooling effectiveness under rotating conditions is much more challenging compared to the detailed heat transfer measurements in confined channels as presented above. Film cooling, by definition is involved with a mainstream flow and a secondary stream of coolant film. With an added effect of rotation, the data acquisition becomes very challenging, and, hence, the research in this front is very limited, even though this topic is still not fully understood, simply because of the presence of complex factors such as rotor-stator interaction, flow modification under the rotation influence and inherent complex interaction between the ejected coolant from the film hole with the mainstream flow. One unique facility at the Turbomachinery Performance and Flow Research Laboratory at TAMU, directed by Schobeiri et al. (e.g., [48]), has the capability of producing detailed adiabatic film cooling effectiveness data on turbine blades under high-speed rotation using the PSP technique.

Figure 13 shows the three-stage turbine facility on which film cooling experiments can be carried out on blade tip for different leakage configurations using PSP technique. The camera, strobe light and associated data acquisition systems were all synced together through an optical sensor such that same angular position can be detected. At 2550 rpm, a 17 μ s camera exposure time was used to capture the image of the blade tip, to process the overall images acquired during the experiment. The pixel's intensity was converted to pressure values using a known calibration relationship, where the PSP calibration was performed separately. More studies on rotating film cooling are presented later.

3.3. Rotor-Stator Disc Cavity Heat Transfer Research

The third part of the experimental facility section is based on the experiments carried out on model axial-flow turbines featuring single or multi-stage turbine sections, where local heat transfer measurements were made on the rotor disc and adjacent stator. One of the first few studies employing liquid crystals to measure radial variation of convective heat transfer coefficient on rotor and stator surfaces was by Bunker et al. [49], although the

detailed measurements were not presented. A one-dimensional semi-infinite conduction model with Duhamel’s superposition principle was used to model the heat diffusion into the solid where heat transfer coefficient was to be determined. There have been other similar investigations that have employed liquid crystals in disc cavity heat transfer research, but the experimental setups are not described here in the interest of brevity, e.g., [50–52].

Lock et al. [53] carried out transient liquid crystal experiments on a model rotor-stator disc cavity where a fraction of the pre-swirl air exiting from the stator was fed to the receiver holes on the rotor disc. The influence of the swirl parameter, rotational Reynolds number and turbulence was investigated using a transient technique developed by Gillespie et al. [54] at the University of Oxford (Figure 14).

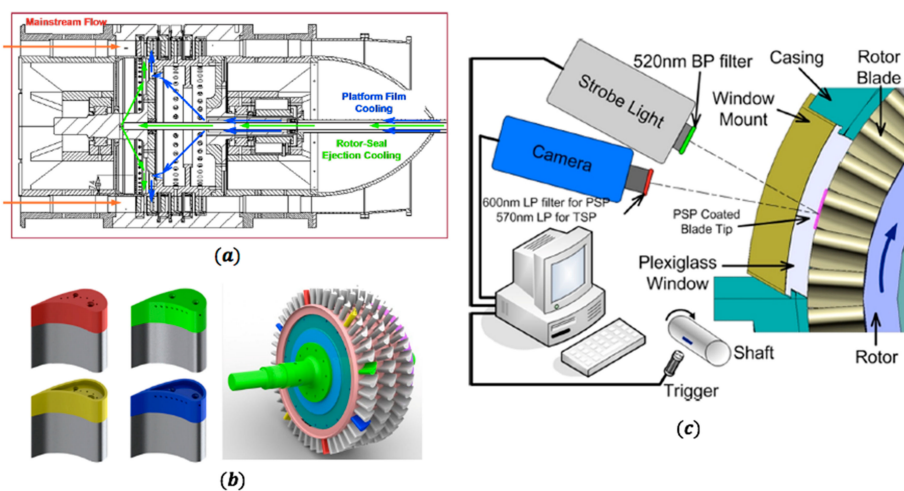


Figure 13. (a) Rotating rig at Turbomachinery Performance and Flow Research Laboratory at TAMU, (b) different blade tip cooling designs, (c) film cooling measurement setup based on PSP [48]. Reprint with permission from ASME (order number 1084748).

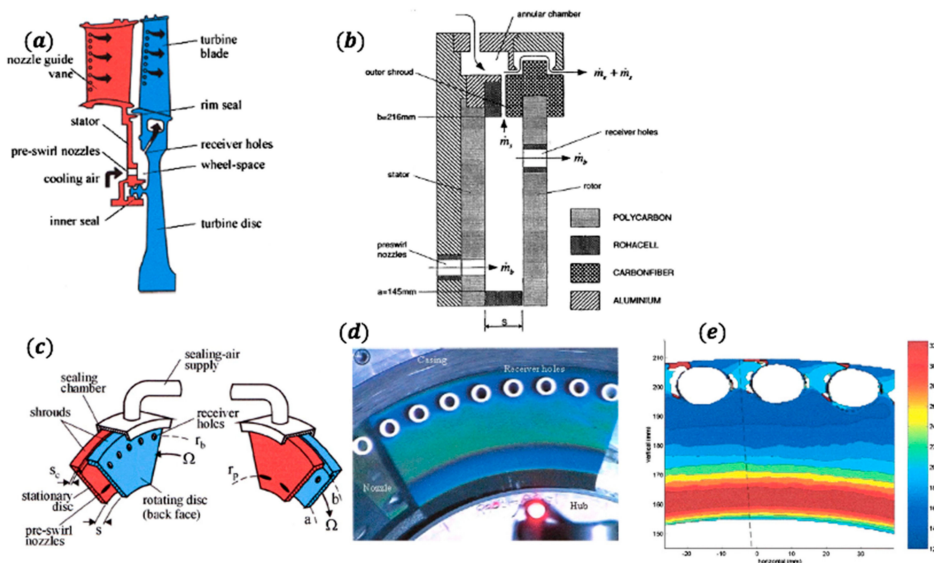


Figure 14. (a) Typical pre-swirl flow system, (b) test-section cross-section, (c) schematic of the test section, (d) sample liquid crystal color change snapshot during the experiment, (e) local heat transfer coefficient map in the vicinity of receiver holes and the azimuthally symmetric nature in the radially inboard regions. [53]. Reprint with permission from ASME (order number 1084749).

4. Experimental Results on Detailed Local Heat Transfer Behavior

This section presents findings of some key experimental investigations on different cooling segments on internal cooling, external cooling, and disc cooling.

4.1. Blade Internal Cooling

As shown in Figure 3, the blade internal cooling can be broadly divided into leading edge, mid-chord region and trailing edge. There has been extensive research in each of these segments and some representative studies have been presented here to capture important findings and to showcase the capability of select few studies in accurately determining the detailed heat transfer quantities under rotating conditions.

4.1.1. Leading Edge/Jet Impingement under Rotation

Lamont et al. [42] investigated leading edge heat transfer characteristics for a single row of five jets under maximum crossflow condition. The impingement orientation with respect to the rotation vector and a sample detailed map of h has been shown in Figure 15. Under rotating conditions, the jets retained their typical stagnation-based heat transfer enhancement profile and that the stationary case heat transfer was in between the trailing and leading-edge rotation scenarios.

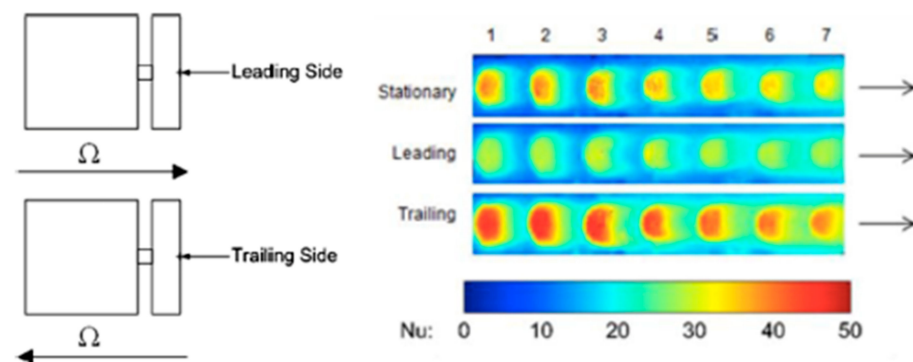


Figure 15. Leading edge jet impingement and detailed Nusselt number map under rotating conditions [40].

One other study on jet impingement on the same facility was carried out by Singh and Ekkad [55,56] for array of small jets impinging on three different dimpled configurations under maximum crossflow condition. Another leading-edge jet impingement with bleed holes was presented by Cocchi et al. [57] where the authors used transient liquid crystal thermography technique to measure local heat transfer in an impingement channel which closely represented the actual blade leading edge profile.

4.1.2. Mid-Chord Cooling: Serpentine Smooth and Roughened Channels

As shown in Figure 3, the mid-chord section of the gas turbine blade features serpentine passages connected to each other by 180-degree bends. The bend that is towards blade tip is flat in shape and the bend towards the blade root is U-shaped. These designs of bends are driven by the geometrical constraints of the blade profile. This section is divided into three more categories: (a) smooth channels and rib-roughened channels, (b) U-bend, and (c) channels featuring other roughness elements.

Smooth and Rib-Roughened Channels

Detailed Sherwood number ratio for rotating smooth channel was presented by authors in [35] (Figure 9). Following this benchmark study, Nikitopoulos et al. [58] and Kim et al. [59] also successfully implemented mass transfer methods under rotating conditions. Lamont et al. [37] presented local Nusselt number ratio for both smooth and ribbed channels under rotating conditions. In the smooth channels, with the help of LC thermography,

the fine details of flow separation in the bend region could be identified under the rotating conditions and how leading and trailing sides were different from each other. For the ribbed channels, the bend heat transfer was not very affected by rotation; however, the leading and trailing side heat transfer was very different for both radially outward and inward channels (Figure 16). A developing channel flow study [41] was also reported by same authors in [37], where different rib profiles were investigated under rotating conditions. Mayo et al. [47] carried out liquid crystal thermography experiments using steady-state heat transfer technique on 90-degree rib roughened ducts. The heat transfer contours were quite different from the LC-based studies that produces sharp images with high contrast highlighting finest of the details. In steady-state experiments, the diffused nature of heat transfer can be observed, since most of the times, the lateral heat diffusion is not corrected. This is one major problem that LC-based studies take care of since the short duration transient experiments on low thermal conductivity and low thermal diffusivity solids result in strictly one-dimensional heat transfer for properly designed experiments. As mentioned earlier, the rotation studies carried out by using Infrared thermography where a steady-state temperature of wall is maintained, has several advantages over typical transient experiments, where the thermo-physical properties are also time variant and buoyancy effects are not properly captured.

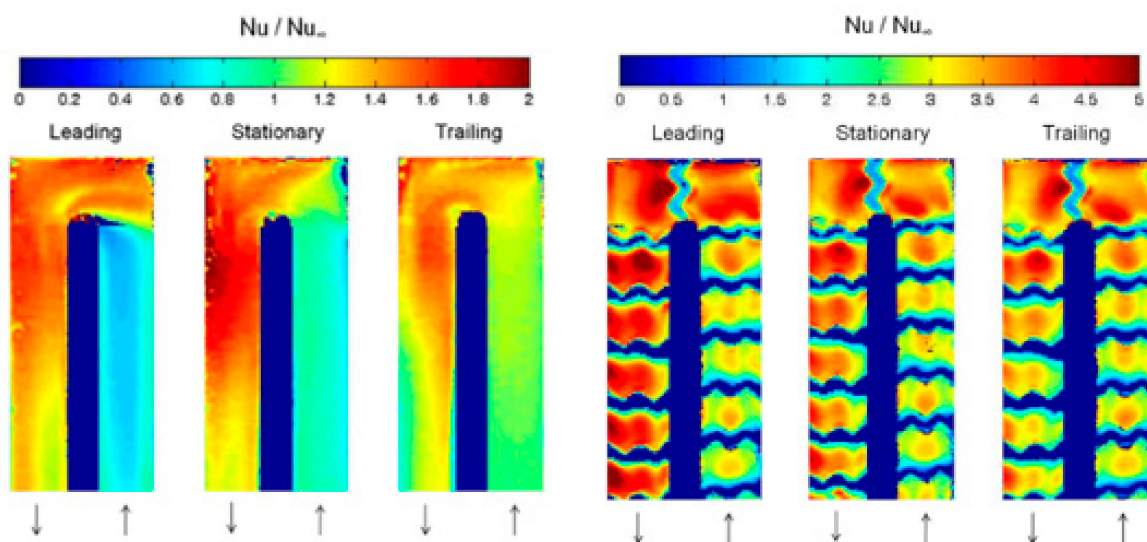


Figure 16. Detailed Nusselt number ratio (Nu/Nu_0) for smooth and W-shaped ribbed channels under stationary and rotating conditions [40].

Chang et al. [60] investigated developing flow in a rotating parallelogram-shaped channel featuring angled rib turbulators. The experiments were carried out over Rotation numbers from 0 to 0.3 and Buoyancy number from 0.002 to 0.23. The wide spectrum of Rotation number and Buoyancy parameters provided a much-needed correlations for leading and trailing side heat transfer under rotating conditions. The same group went on to publish several research articles covering different aspects of rotating heat transfer for a wide variety of configurations such as, two opposite walls roughened by skewed ribs [61], impinging jet-row [62], S-shaped zig-zag channel [63], furrowed channel with opposite skewed sinusoidal wavy walls [64], attached and detached transverse ribs [65] and twin-pass smooth-walled parallelogram channels [66].

The above investigations using advanced thermal diagnostics yielding detailed convective heat transfer coefficient measurements provide valuable insight into the complex flow and thermal transport mechanisms. The interplay of Coriolis force, centrifugal buoyancy, rotation-assisted near-wall turbulence, Reynolds number etc. requires the knowledge of detailed heat transfer measurements along with flow-field measurements using particle-image velocimetry, e.g., [67–70]. With improved understanding of transport phenomena

under rotating conditions, it is also imperative to utilize this knowledge database in the development of efficient cooling designs that have higher thermal hydraulic performance and where rotation-induced detrimental effects can be negated. To this end, some of the recent investigations by Singh and Ekkad [16,71–73] are mentioned here.

Singh et al. [16] performed transient liquid crystal thermography experiments to develop cooling designs where rotation was used in favor of heat transfer enhancement on both leading and trailing walls. In the conventional two-passage channels featuring rib turbulators, the flow is radially outward in the first passage and radially inward in the second passage. The combined effects of Coriolis force and centrifugal buoyancy forces on this arrangement of coolant flow in 1st and 2nd passages result in enhancement in heat transfer on trailing walls and leading walls, respectively, and reduction in heat transfer on the leading and trailing walls of the 1st and 2nd passages. This redistribution of convective heat transfer coefficient not only deviates from the Nusselt number ratio levels obtained under stationary conditions, but it also results in non-uniformity in the blade temperature, which leads to increase in thermal stresses. These thermal stresses when combined with the rotational effects, can result in frequent maintenance of the turbine blade or may even lead to a permanent failure. Hence, it is imperative to somehow damp the detrimental effects of rotation or utilize it in an intelligent way. The cooling channel orientations presented in Figure 17 essentially results in heat transfer enhancement for both radially outward and inward flows, where maximum benefit can be seen in the 2nd passage, where leading wall heat transfer was enhanced.

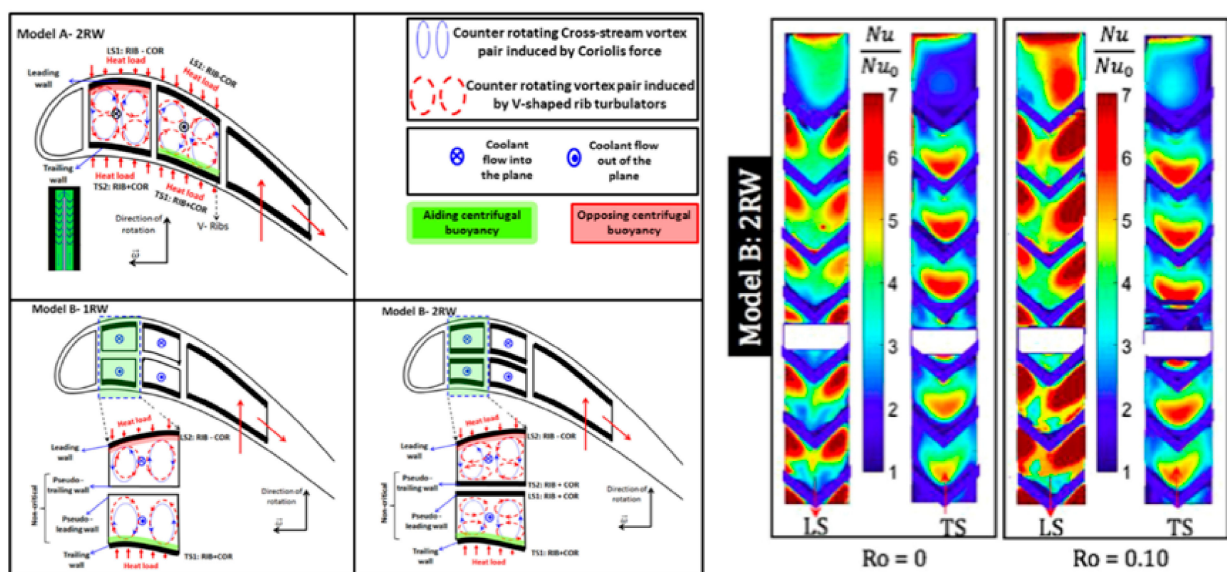


Figure 17. Novel cooling configurations utilizing rotation in favor of heat transfer enhancement on both leading and trailing sides [16]. Reprint with permission from Elsevier (order number 4961580086797).

A series of experiments were performed by Singh et al. [71–73] to develop multi-passage serpentine passages that could essentially negate the detrimental effects of Coriolis force on heat transfer in the conventional orthogonally oriented channels. In [71], the authors presented an experimental and numerical study on four- and six-passage smooth configurations where the passages were arranged parallel to the rotation vector with an aim to negate the Coriolis force effect on flow and heat transfer. The authors successfully demonstrated the efficacy of this concept in meeting the above desired goal through presentation of detailed heat transfer measurements with high degree of similarity between rotating and stationary conditions even at the local scale (Figure 18).

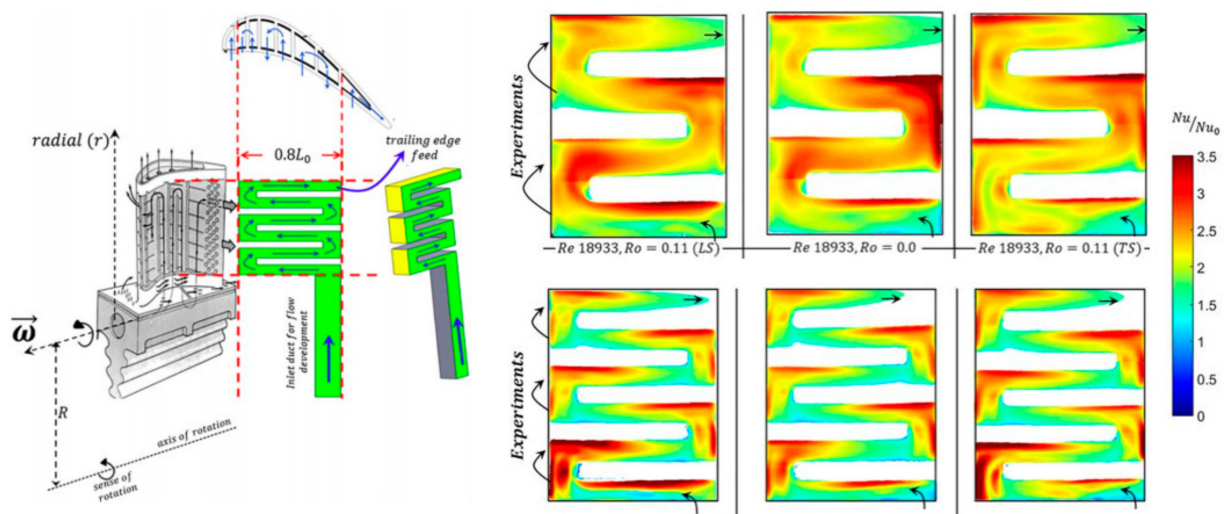


Figure 18. Parallel rotation multi-passage cooling scheme proposed by Singh et al. [71]. Reprint with permission from ASME (order number 1085964).

In a follow-up paper [72], the same authors [71] extended this concept to channels featuring 45-degree angled rib turbulators and showed that the concept worked for rough channels as well (Figure 19). An eight-passage smooth duct was also presented in this series of papers on the concept of negating Coriolis force effect [73].

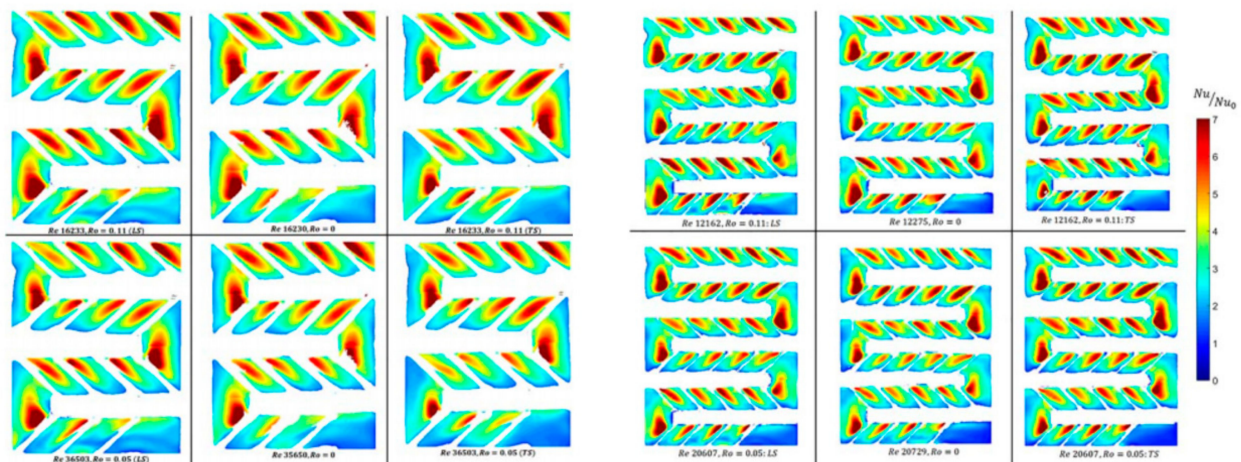


Figure 19. Parallel rotation multi-passage ribbed configurations proposed by Singh et al. [72]. Reprint with permission from ASME (order number 1085960).

U-bend

Iacovides et al. [74] carried out an experimental study using TLCT on a rotating square-ended U-bend where the channel cross-sectional area changed across the bend region and a wide range of Prandtl number was also studied. It was found that post the bend region, the flow separation effects were lower for water when compared to air. Another study by Iacovides et al. [75] reported U-bend heat transfer where the passages were equipped with 45-degree angled rib turbulators. Some of the prior studies mentioned above have also explored the U-bend heat transfer and provide important discussion on flow separation at the divider wall [17], impingement effect on the blade tip underside corresponding to the 1st passage [17], effect of Dean-type vortices [17], and post-bend heat and flow characteristics [16,17].

Other Roughness Elements Used in Mid-Chord Region

Dimples (concavities) and protrusions are also widely investigated for their potential application in cooling mid-chord serpentine passages. These roughness elements are known to produce relatively lower heat transfer compared to rib turbulators; however, the concomitant pressure drop is also low. For detailed investigations on such concepts, the reader is referred to some stationary condition studies [13,14,76–78]. In this subsection, we are highlighting some representative investigations on detailed heat transfer on dimple/protrusion channels. Kim et al. [79] investigated the effect of dimple depth, dimple center-to-center distance, channel height on heat transfer coefficient for wide range of Reynolds number at a fixed rotational speed of 500 rpm. Kim et al. [80] investigated dimpled-channel orientation effects on heat transfer for different rotation numbers. Hemispherical protrusions in a channel were investigated by Chang et al. [81] for Rotation numbers between 0–0.6. Chang et al. [82] also investigated rib-dimpled compound channel under rotating conditions.

Blade Trailing-Edge Cooling

As shown in Figure 3, the blade trailing edge is typically cooled with an array of pin-fins. Under stationary conditions, pin-fin heat transfer for various pin shapes is well characterized through detailed heat/mass transfer measurements [83–86]. For trailing edge cooling under rotation, the flow is radially outward, and the pin-fins are fabricated in a single channel. Chang et al. [87] investigated heat transfer characteristics of diamond-shaped pin-fins arranged in a staggered form for Rotation numbers between 0 and 0.6. Huang et al. [46] investigated rotating heat transfer characteristics of channel featuring inline and staggered arrangements on pin-fins. Typical local Nusselt number contour is presented in Figure 20, where the trailing side enhancement can be clearly observed over the leading side.

This trend indicates that the combined effects of Coriolis force and centrifugal buoyancy forces in radially outward channel that results in transport of relatively colder fluid from channel core to the trailing side wall is strong and present in many different roughened channels. Another study by the same leading author [88] focused on radially rotating rectangular channel with compound cooling concept of pin-fins on skewed rib lands. Compound cooling scheme of protrusion and pin in radially outward flow single channel was investigated by Ullal et al. [89]. Some parametric studies on trailing edge cooling with pin-fins were reported in [90,91]. Pagnacco et al. [92] investigated a unique configuration with coolant fed to the pin-fin channel via a serpentine rib-roughened duct. The Rotation number was very low to notice any discernable differences between pressure and suction side internal heat transfer characteristics.

4.2. Blade External Cooling

Blade external cooling is an extremely challenging task due to the complex nature of tip leakage flows, the rotation assisted- and rotor-stator-interaction-enabled flow disturbances, leakage flows emanating from the rotor-stator disc cavity modifying the blade platform fluid dynamics, etc. The tip of a blade is usually cooled both internally and externally. The internal side of a blade tip lies in the U-bend region of the serpentine passages with a flat tip. One cooling scheme based on micro-scale roughness elements on the blade tip underside was investigated by Ledezma and Bunker [93] using liquid crystal thermography under stationary condition. A detailed summary on stationary heat transfer measurements around blade tip region can be found in the review article by Xie and Sunden [94]. In this section, only a select few studies on rotating heat transfer measurements for blade tip/platform (external) are presented.

Suryanarayanan et al. [95] were the first to present detailed adiabatic film cooling measurements on blade endwall with purge air emanating from the disc cavity, on a three-stage axial flow turbine facility. A pressure sensitive paint-based technique was used to find adiabatic film cooling effectiveness.

Rezasoltani et al. [47] carried out an experimental and numerical study on blade tip film cooling under rotating conditions. The measurements were made on the same facility as in [95] and the technique is presented earlier in this paper (Section 3.2). Blade tip and shroud heat transfer coefficient and adiabatic film cooling effectiveness measurements under rotating conditions was investigated recently by Tamunobere and Acharya [96,97] where the authors used transient liquid crystal thermography technique to find both heat transfer and adiabatic film cooling effectiveness. The details of this technique can be found in [98,99].

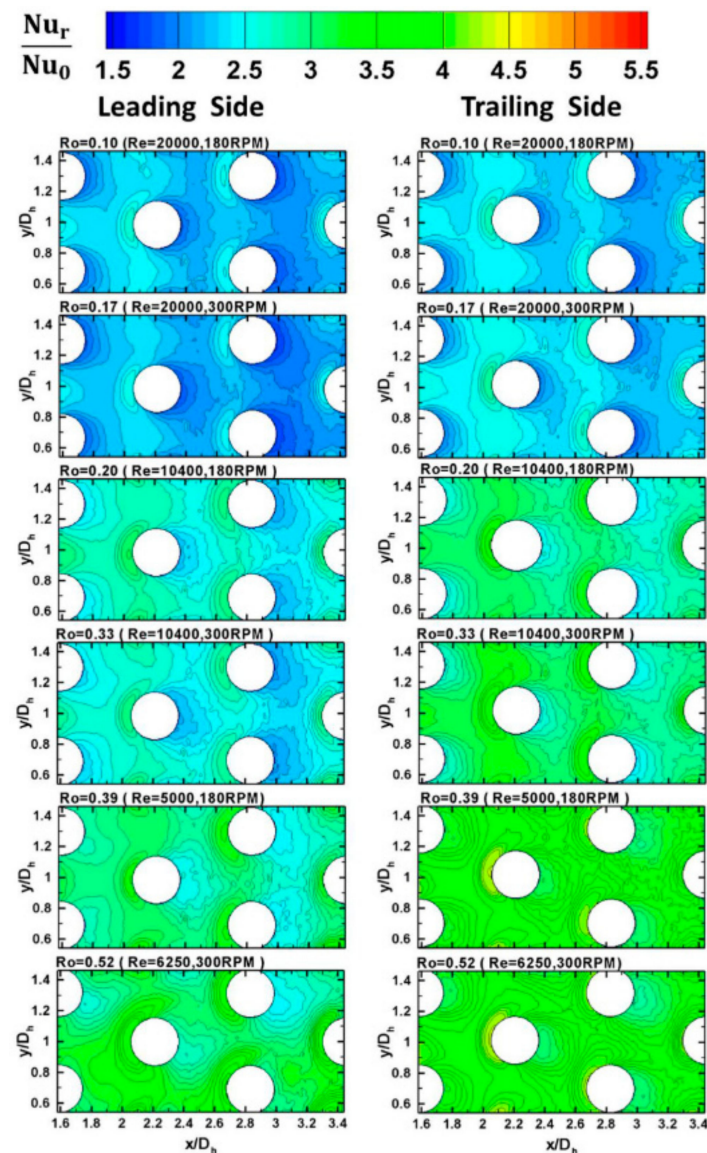


Figure 20. Local Nusselt number under rotation [46]. Reprint with permission from Elsevier (order number 4970940401126).

4.3. Rotor-Stator Disc Cavity Cooling

Due to the circumferential sinusoidal pressure variation at the tip of the rotor-stator disc cavity, there is an unsteady hot gas ingestion into the disc cavity that has the potential to significantly shorten the component lifespan. Extensive research has been conducted over the past three decades to understand the ingestion and egress mechanisms in the disc cavity, and several semi-empirical models have been proposed. Some recent models have proven their robustness after being tested with large volumes of existing static pressure measurements in disc cavity and blade platform and tracer gas ingestion measurements

in the cavity. These models can predict the ingestion and egress flow rates for different test conditions, such as main airflow Reynolds number, Rotational Reynolds number, turbulence parameter, purge air flow rates etc. [100–113].

In this section, we focus on some key studies employing advanced thermal diagnostics to measure local heat transfer coefficient in the rotor-stator disc cavity. Earlier studies in the late 1980s and early 1990s by the group at Arizona State University successfully demonstrated the use of liquid crystals in transient experiments to measure the radial variation of Nusselt number in rotating systems, e.g., [48–51]. Later, the studies conducted at the University of Bath (UK) demonstrated the use of liquid crystals thermography in measuring the local heat transfer characteristics of wide range of disc cavity configurations with purge flows. The details of this technique are presented in [114,115] and a detailed analysis of associated uncertainties in liquid crystal transient technique is given in [116].

Further, more recently, the effect of ingress on the disc temperature was studied using liquid crystals by [117]. More studies employing these advanced thermal diagnostics are expected as they provide great insight into the local heat transfer characteristics of surfaces in the rotating framework and provide extensive validation to the numerical efforts.

5. Concluding Remarks

This review article presents the employment of advanced thermal diagnostic techniques for detailed heat transfer measurements under complex rotating systems pertaining to high-pressure gas turbine stages. The popular techniques based on heat/mass transfer have been briefly presented. The experimental facilities which have successfully demonstrated the use of advanced thermal diagnostics have been presented in detail. The review was focused on three major categories: (1) turbine blade internal cooling, (2) turbine blade external cooling, and (3) rotor-stator disc cavity cooling. The experimental methods and the measurement techniques have been critically assessed for their accuracy and robustness. Overall, the knowledge database generated through these techniques under rotating conditions provide extremely valuable insights into the complex internal and external flow scenarios which are typical of gas turbine hot gas path. These investigations provide guidance to engineers and researchers in the design of cooling concepts for next generation aircraft and land-based power generation gas turbines. With the continued advancements in the resolution and accuracy of the measurement devices and the need for validation of large-eddy simulation-based numerical predictions, more studies utilizing the advanced thermal diagnostics can be expected for which this article may serve as a reference tool.

Author Contributions: S.V.E.: conceptualization; writing—review and editing; supervision; project administration, P.S.: methodology; writing—original draft preparation. Both the authors have read and agreed to the published version of the manuscript.

Funding: This research received no external funding.

Conflicts of Interest: The authors declare no conflict of interest.

References

1. Han, J. Fundamental Gas Turbine Heat Transfer. *ASME J. Therm. Sci. Eng. Appl.* **2013**, *5*, 021007. [[CrossRef](#)]
2. Han, J.C.; Wright, L.M. Enhanced Internal Cooling of Turbine Blades and Vanes. In *The Gas Turbine Handbook*; U.S. DOE, National Energy Technology Laboratory: Morgantown, WV, USA, 2007; pp. 321–352.
3. Han, J.-C.; Dutta, S.; Ekkad, S.V. *Gas Turbine Heat Transfer and Cooling Technology*; CRC Press: Boca Raton, FL, USA, 2012.
4. Mhetras, S.; Narzary, D.; Gao, Z.; Han, J.C. Effect of a Cutback Squealer and Cavity Depth on Film-Cooling Effectiveness on a Gas Turbine Blade Tip. *ASME J. Turbomach.* **2008**, *130*, 021002. [[CrossRef](#)]
5. Sangan, C.M.; Pountney, O.J.; Zhou, K.; Wilson, M.; Michael Owen, J.; Lock, G.D. Experimental Measurements of Ingestion Through Turbine Rim Seals—Part I: Externally Induced Ingress. *ASME J. Turbomach.* **2013**, *135*, 021012. [[CrossRef](#)]
6. Phadke, U.P.; Owen, J.M. Aerodynamic aspects of the sealing of gas-turbine rotor-stator systems: Part 1: The behavior of simple shrouded rotating-disk systems in a quiescent environment. *Int. J. Heat Fluid Flow* **1988**, *9*, 98–105. [[CrossRef](#)]
7. Bohn, D.; Johann, E.; Krüger, U. Experimental and Numerical Investigations of Aerodynamic Aspects of Hot Gas Ingestion in Rotor-Stator Systems with Superimposed Cooling Mass Flow. In Proceedings of the ASME 1995 International Gas Turbine and Aeroengine Congress and Exposition. Volume 1: Turbomachinery, Houston, TX, USA, 5–8 June 1995; p. V001T01A034. [[CrossRef](#)]

8. Ireland, P.T.; Jones, T.V. Liquid crystal measurements of heat transfer and surface shear stress. *Meas. Sci. Technol.* **2000**, *11*, 969. [[CrossRef](#)]
9. Ekkad, S.V.; Han, J.C. A transient liquid crystal thermography technique for gas turbine heat transfer measurements. *Meas. Sci. Technol.* **2000**, *11*, 957. [[CrossRef](#)]
10. Camci, C.; Kim, K.; Hippensteele, S.A.; Poinsette, P.E. Evaluation of a hue capturing based transient liquid crystal method for high-resolution mapping of convective heat transfer on curved surfaces. *J. Heat Transfer.* **1993**, *115*, 311–318. [[CrossRef](#)]
11. Hay, J.L.; Hollingsworth, D.K. A comparison of trichromic systems for use in the calibration of polymer-dispersed thermochromic liquid crystals. *Exp. Therm. Fluid Sci.* **1996**, *12*, 1–12. [[CrossRef](#)]
12. Singh, P.; Ekkad, S. Experimental study of heat transfer augmentation in a two-pass channel featuring V-shaped ribs and cylindrical dimples. *Appl. Therm. Eng.* **2017**, *116*, 205–216. [[CrossRef](#)]
13. Gomez Ramirez, D. Heat Transfer and Flow Measurements in an Atmospheric Lean Pre-Mixed Combustor. Ph.D. Thesis, Virginia Tech, Blacksburg, VA, USA, 2016.
14. Singh, P.; Pandit, J.; Ekkad, S.V. Characterization of heat transfer enhancement and frictional losses in a two-pass square duct featuring unique combinations of rib turbulators and cylindrical dimples. *Int. J. Heat Mass Transf.* **2017**, *106*, 629–647. [[CrossRef](#)]
15. Singh, P.; Ravi, B.V.; Ekkad, S.V. Experimental and numerical study of heat transfer due to developing flow in a two-pass rib roughened square duct. *Int. J. Heat Mass Transf.* **2016**, *102*, 1245–1256. [[CrossRef](#)]
16. Singh, P.; Li, W.; Ekkad, S.V.; Ren, J. A new cooling design for rib roughened two-pass channel having positive effects of rotation on heat transfer enhancement on both pressure and suction side internal walls of a gas turbine blade. *Int. J. Heat Mass Transf.* **2017**, *115*, 6–20. [[CrossRef](#)]
17. Singh, P.; Li, W.; Ekkad, S.V.; Ren, J. Experimental and numerical investigation of heat transfer inside two-pass rib roughened duct (AR= 1: 2) under rotating and stationary conditions. *Int. J. Heat Mass Transf.* **2017**, *113*, 384–398. [[CrossRef](#)]
18. Goldstein, R.J.; Cho, H.H. A review of mass transfer measurements using naphthalene sublimation. *Exp. Therm. Fluid Sci.* **1995**, *10*, 416–434. [[CrossRef](#)]
19. Zhang, L.; Fox, M. Flat Plate Film Cooling Measurements using PSP Gas Chromatograph Techniques. In Proceedings of the Fifth ASME/JSME Joint Thermal Engineering Conference, San Diego, CA, USA, 1 July 1999.
20. Han, J.C.; Rallabandi, A. Turbine blade film cooling using PSP technique. *Front. Heat Mass Transf.* **2010**, *1*, 013001. [[CrossRef](#)]
21. Wright, L.M.; Gao, Z.; Varvel, T.A.; Han, J.C. Assessment of Steady State PSP, TSP, and IR Measurement Techniques for Flat Plate Film Cooling. In Proceedings of the ASME 2005 Summer Heat Transfer Conference Collocated with the ASME 2005 Pacific Rim Technical Conference and Exhibition on Integration and Packaging of MEMS, NEMS, and Electronic Systems. Heat Transfer: Volume 3, San Francisco, CA, USA, 17–22 July 2005; pp. 37–46. [[CrossRef](#)]
22. Epstein, A.H.; Kerrebrock, J.L.; Koo, J.J.; Preiser, U.Z. Rotational effects on impingement cooling. *Heat Transf. Fluid Flow Rotat. Mach.* **1987**, 86–102.
23. Abhari, R.S.; Epstein, A.H. An Experimental Study of Film Cooling in a Rotating Transonic Turbine. *ASME J. Turbomach.* **1994**, *116*, 63–70. [[CrossRef](#)]
24. Abhari, R.S.; Epstein, A.H. An Experimental Study of Film Cooling in a Rotating Transonic Turbine. In Proceedings of the ASME 1992 International Gas Turbine and Aeroengine Congress and Exposition. Volume 4: Heat Transfer, Electric Power, Industrial and Cogeneration, Cologne, Germany, 1–4 June 1992; p. V004T09A018. [[CrossRef](#)]
25. Wagner, J.H.; Johnson, B.V.; Kopper, F.C. Heat Transfer in Rotating Serpentine Passages with Smooth Walls. *ASME J. Turbomach.* **1991**, *113*, 321–330. [[CrossRef](#)]
26. Johnson, B.V.; Wagner, J.H.; Steuber, G.D.; Yeh, F.C. Heat Transfer in Rotating Serpentine Passages with Selected Model Orientations for Smooth or Skewed Trip Walls. *ASME J. Turbomach.* **1994**, *116*, 738–744. [[CrossRef](#)]
27. Bonhoff, B.; Parneix, S.; Leusch, J.; Johnson, B.V.; Schabacker, J.; Bölcs, A. Experimental and numerical study of developed flow and heat transfer in coolant channels with 45 degree ribs. *Int. J. Heat Fluid Flow* **1999**, *20*, 311–319. [[CrossRef](#)]
28. Johnson, B.V.; Wagner, J.H.; Steuber, G.D. *Effects of Rotation on Coolant Passage Heat Transfer. Volume 2: Coolant Passages with Trips Normal and Skewed to the Flow*; NASA Contractor Report # 4396; NASA: Washington, DC, USA, 1993.
29. Han, J.C.; Zhang, Y.M.; Lee, C.P. Influence of surface heating condition on local heat transfer in a rotating square channel with smooth walls and radial outward flow. *J. Turbomach.* **1994**, *116*, 149–158. [[CrossRef](#)]
30. Parsons, J.A.; Han, J.-C.; Zhang, Y. Effect of model orientation and wall heating condition on local heat transfer in a rotating two-pass square channel with rib turbulators. *Int. J. Heat Mass Transf.* **1995**, *38*, 1151–1159. [[CrossRef](#)]
31. Han, J.-C.; Zhang, Y.-M.; Kalkuehler, K. Uneven Wall Temperature Effect on Local Heat Transfer in a Rotating Two-Pass Square Channel with Smooth Walls. *ASME J. Heat Transf.* **1993**, *115*, 912–920. [[CrossRef](#)]
32. Taslim, M.E.; Bondi, L.A.; Kercher, D.M. An Experimental Investigation of Heat Transfer in an Orthogonally Rotating Channel Roughened With 45 deg Criss-Cross Ribs on Two Opposite Walls. *J. Turbomach.* **1991**, *113*, 346–353. [[CrossRef](#)]
33. Bons, J.P.; Kerrebrock, J.L. Complementary Velocity and Heat Transfer Measurements in a Rotating Cooling Passage with Smooth Walls. In Proceedings of the ASME 1998 International Gas Turbine and Aeroengine Congress and Exhibition, Volume 4: Heat Transfer; Electric Power; Industrial and Cogeneration, Stockholm, Sweden, 2–5 June 1998; p. V004T09A080. [[CrossRef](#)]
34. Dunn, M.G. Phase and Time-Resolved Measurements of Unsteady Heat Transfer and Pressure in a Full-Stage Rotating Turbine. *ASME J. Turbomach.* **1990**, *112*, 531–538. [[CrossRef](#)]

35. Park, C.W.; Lau, S.C. Effect of Channel Orientation of Local Heat (Mass) Transfer Distributions in a Rotating Two-Pass Square Channel with Smooth Walls. *J. Heat Transf.* **1998**, *120*, 624–632. [[CrossRef](#)]
36. Chang, S.W.; Liou, T.-M.; Po, Y. Coriolis and rotating buoyancy effect on detailed heat transfer distributions in a two-pass square channel roughened by 45° ribs at high rotation numbers. *Int. J. Heat Mass Transf.* **2010**, *53*, 1349–1363. [[CrossRef](#)]
37. Blair, M.F.; Wagner, J.H.; Steuber, G.D. New applications of liquid-crystal thermography in rotating turbomachinery heat transfer research. In Proceedings of the ASME, 36th International Gas Turbine and Aeroengine Congress and Exposition, Orlando, FL, USA, 3–6 June 1991.
38. El-Husayni, H.A.; Taslim, M.E.; Kercher, D.M. Experimental Heat Transfer Investigation of Stationary and Orthogonally Rotating Asymmetric and Symmetric Heated Smooth and Turbulated Channels. *ASME J. Turbomach.* **1994**, *116*, 124–132. [[CrossRef](#)]
39. Lamont, J.A.; Ekkad, S.V.; Alvin, M.A. Detailed Heat Transfer Measurements Inside Rotating Ribbed Channels Using the Transient Liquid Crystal Technique. *ASME J. Sci. Eng. Appl.* **2012**, *4*, 011002. [[CrossRef](#)]
40. Lamont, J.A. Heat Transfer in Stationary and Rotating Coolant Channels Using a Transient Liquid Crystal Technique. Ph.D. Thesis, Virginia Tech, Blacksburg, VA, USA, 2012.
41. Lamont, J.A.; Ekkad, S.V.; Alvin, M.A. Effect of Rotation on Detailed Heat Transfer Distribution for Various Rib Geometries in Developing Channel Flow. *ASME J. Heat Transf.* **2013**, *136*, 011901. [[CrossRef](#)]
42. Lamont, J.A.; Ekkad, S.V.; Alvin, M.A. Effects of Rotation on Heat Transfer for a Single Row Jet Impingement Array with Crossflow. *ASME J. Heat Transf.* **2012**, *134*, 082202. [[CrossRef](#)]
43. Burberi, E.; Massini, D.; Cocchi, L.; Mazzei, L.; Andreini, A.; Facchini, B. Effect of Rotation on a Gas Turbine Blade Internal Cooling System: Numerical Investigation. *ASME J. Turbomach.* **2016**, *139*, 031005. [[CrossRef](#)]
44. Kulkarni, A. Characterization of Heat Transfer in Serpentine Passages Using Thermochromic Liquid Crystals. Master's Thesis, The Ohio State University, Columbus, OH, USA, 2018.
45. Waidmann, C.; Poser, R.; Nieland, S.; Wolfersdorf, J. Design of A Rotating Test Rig for Transient Thermochromic Liquid Crystal Heat Transfer Experiments. In Proceedings of the International Symposium on Transport Phenomena and Dynamics of Rotating Machinery (ISROMAC), Hawaii, HI, USA, 10–15 April 2016. Available online: <https://hal.archives-ouvertes.fr/hal-01884257/document> (accessed on 18 December 2020).
46. Huang, S.-C.; Wang, C.-C.; Liu, Y.-H. Heat transfer measurement in a rotating cooling channel with staggered and inline pin-fin arrays using liquid crystal and stroboscopy. *Int. J. Heat Mass Transf.* **2017**, *115*, 364–376. [[CrossRef](#)]
47. Mayo, I.; Lahalle, A.; Gori, G.L.; Arts, T. Aerothermal Characterization of a Rotating Ribbed Channel at Engine Representative Conditions—Part II: Detailed Liquid Crystal Thermography Measurements. *ASME J. Turbomach.* **2016**, *138*, 101009. [[CrossRef](#)]
48. Rezasoltani, M.; Lu, K.; Schobeiri, M.T.; Han, J.-C. A Combined Experimental and Numerical Study of the Turbine Blade Tip Film Cooling Effectiveness under Rotation Condition. *ASME J. Turbomach.* **2015**, *137*, 051009. [[CrossRef](#)]
49. Bunker, R.S.; Metzger, D.E.; Wittig, S. Local Heat Transfer in Turbine Disk Cavities: Part I—Rotor and Stator Cooling With Hub Injection of Coolant. *ASME J. Turbomach.* **1992**, *114*, 211–220. [[CrossRef](#)]
50. Roy, R.P.; Xu, G.; Feng, J. A Study of Convective Heat Transfer in a Model Rotor–Stator Disk Cavity. *ASME J. Turbomach.* **2001**, *123*, 621–632. [[CrossRef](#)]
51. Bunker, R.S.; Metzger, D.E.; Wittig, S. Local Heat Transfer in Turbine Disk Cavities: Part II—Rotor Cooling with Radial Location Injection of Coolant. *ASME J. Turbomach.* **1992**, *114*, 221–228. [[CrossRef](#)]
52. Metzger, D.E.; Bunker, R.S.; Bosch, G. Transient Liquid Crystal Measurement of Local Heat Transfer on a Rotating Disk with Jet Impingement. *ASME J. Turbomach.* **1991**, *113*, 52–59. [[CrossRef](#)]
53. Lock, G.D.; Wilson, M.; Owen, J.M. Influence of Fluid Dynamics on Heat Transfer in a Preswirl Rotating-Disk System. *ASME J. Eng. Gas. Turbines Power* **2004**, *127*, 791–797. [[CrossRef](#)]
54. Gillespie, D.R.H.; Wang, Z.; Ireland, P.T.; Kohler, S.T. Full Surface Local Heat Transfer Coefficient Measurements in a Model of an Integrally Cast Impingement Cooling Geometry. *ASME J. Turbomach.* **1998**, *120*, 92–99. [[CrossRef](#)]
55. Singh, P.; Ekkad, S. Effects of Rotation on Heat Transfer due to Jet Impingement on Cylindrical Dimpled Target Surface. In Proceedings of the ASME Turbo Expo 2016: Turbomachinery Technical Conference and Exposition. Volume 5B: Heat Transfer, Seoul, Korea, 13–17 June 2016; V05BT16A010. [[CrossRef](#)]
56. Singh, P.; Ekkad, S.V. Detailed Heat Transfer Measurements of Jet Impingement on Dimpled Target Surface under Rotation. *ASME J. Sci. Eng. Appl.* **2018**, *10*, 031006. [[CrossRef](#)]
57. Cocchi, L.; Facchini, B.; Picchi, A. Heat Transfer Measurements in Leading-Edge Cooling Geometry under Rotating Conditions. *J. Heat Transf.* **2019**, *33*, 844–855. [[CrossRef](#)]
58. Nikitopoulos, D.E.; Eliades, V.; Acharya, S. Heat Transfer Enhancements in Rotating Two-Pass Coolant Channels with Profiled Ribs: Part 2—Detailed Measurements. *J. Turbomach.* **2000**, *123*, 107–114. [[CrossRef](#)]
59. Kim, K.M.; Kim, Y.Y.; Lee, N.H.; Rhee, D.H.; Cho, H.H. Local Heat/Mass Transfer Phenomena in Rotating Passage, Part 1: Smooth Passage. *J. Heat Transf.* **2006**, *20*, 188–198. [[CrossRef](#)]
60. Chang, S.W.; Liou, T.-M.; Lee, T.-H. Thermal performance of developing flow in a radially rotating parallelogram channel with 45° ribs. *Int. J. Sci.* **2012**, *52*, 186–204. [[CrossRef](#)]
61. Chang, S.; Chiang, K.; Kao, J. Heat transfer in rotating spiral channel with two opposite planar walls roughened by skew ribs. *Int. J. Sci.* **2012**, *56*, 107–121. [[CrossRef](#)]

62. Chang, S.; Yu, K.-C. Thermal performance of radially rotating trapezoidal channel with impinging jet-row. *Int. J. Heat Mass Transf.* **2019**, *136*, 246–264. [[CrossRef](#)]
63. Chang, S.W.; Wu, P.-S.; Chen, C.-S.; Weng, C.-C.; Jiang, Y.-R.; Shih, S.-H. Thermal performance of radially rotating two-pass S-shaped zig-zag channel. *Int. J. Heat Mass Transf.* **2017**, *115*, 1011–1031. [[CrossRef](#)]
64. Chang, S.; Lees, A.; Liou, T.-M.; Hong, G. Heat transfer of a radially rotating furrowed channel with two opposite skewed sinusoidal wavy walls. *Int. J. Sci.* **2010**, *49*, 769–785. [[CrossRef](#)]
65. Liou, T.-M.; Chang, S.W.; Lan, Y.A.; Chan, S.P.; Liu, Y.S. Heat Transfer and Flow Characteristics of Two-Pass Parallelogram Channels with Attached and Detached Transverse Ribs. *ASME J. Heat Transf.* **2017**, *139*, 042001. [[CrossRef](#)]
66. Liou, T.-M.; Chang, S.W.; Yang, C.-C.; Lan, Y.-A. Thermal Performance of a Radially Rotating Twin-Pass Smooth-Walled Parallelogram Channel. *ASME J. Turbomach.* **2014**, *136*, 121007. [[CrossRef](#)]
67. Di Sante, A.; Theunissen, R.; Braembussche, R.A.V.D. A new facility for time-resolved PIV measurements in rotating channels. *Exp. Fluids* **2007**, *44*, 179–188. [[CrossRef](#)]
68. Armellini, A.; Casarsa, L.; Mucignat, C. Flow field analysis inside a gas turbine trailing edge cooling channel under static and rotating conditions. *Int. J. Heat Fluid Flow* **2011**, *32*, 1147–1159. [[CrossRef](#)]
69. Elfert, M.; Schroll, M.; Förster, W. PIV Measurement of Secondary Flow in a Rotating Two-Pass Cooling System with an Improved Sequencer Technique. *ASME J. Turbomach.* **2011**, *134*, 031001. [[CrossRef](#)]
70. Mucignat, C.; Armellini, A.; Casarsa, L. Flow field analysis inside a gas turbine trailing edge cooling channel under static and rotating conditions: Effect of ribs. *Int. J. Heat Fluid Flow* **2013**, *42*, 236–250. [[CrossRef](#)]
71. Singh, P.; Ji, Y.; Ekkad, S.V. Multi-Pass Serpentine Cooling Designs for Negating Coriolis Force Effect on Heat Transfer: Smooth Channels. *ASME J. Turbomach.* **2019**, *141*, 1–28. [[CrossRef](#)]
72. Singh, P.; Ji, Y.; Ekkad, S.V. Multi-pass Serpentine Cooling Designs for Negating Coriolis Force Effect on Heat Transfer: 45-deg Angled Rib Turbulated Channels. *ASME J. Turbomach.* **2019**, *141*, 1–24. [[CrossRef](#)]
73. Singh, P.; Sarja, A.; Ekkad, S.V. Experimental and Numerical Study of Chord-Wise Eight-Passage Serpentine Cooling Design for Eliminating the Coriolis Force Adverse Effect on Heat Transfer. *ASME J. Sci. Eng. Appl.* **2020**, *13*, 1–20. [[CrossRef](#)]
74. Iacovides, H.; Kounadis, D.; Xu, Z. Experimental study of thermal development in a rotating square-ended U-bend. *Exp. Fluid Sci.* **2009**, *33*, 482–494. [[CrossRef](#)]
75. Iacovides, H.; Jackson, D.; Kelemenis, G.; Launder, B.E.; Yuan, Y.-M. Flow and heat transfer in a rotating U-bend with 45° ribs. *Int. J. Heat Fluid Flow* **2001**, *22*, 308–314. [[CrossRef](#)]
76. Ligrani, P.M.; Harrison, J.L.; Mahmmod, G.I.; Hill, M.L. Flow structure due to dimple depressions on a channel surface. *Phys. Fluids* **2001**, *13*, 3442–3451. [[CrossRef](#)]
77. Ligrani, P.M.; Mahmood, G.I.; Harrison, J.L.; Clayton, C.M.; Nelson, D.L. Flow structure and local Nusselt number variations in a channel with dimples and protrusions on opposite walls. *Int. J. Heat Mass Transf.* **2001**, *44*, 4413–4425. [[CrossRef](#)]
78. Na Jang, H.; Park, J.S.; Kwak, J.S. Experimental study on heat transfer characteristics in a ribbed channel with dimples, semi-spherical protrusions, or oval protrusions. *Appl. Eng.* **2018**, *131*, 734–742. [[CrossRef](#)]
79. Kim, S.; Lee, Y.J.; Choi, E.Y.; Kwak, J.S. Effect of Dimple Configuration on Heat Transfer Coefficient in a Rotating Channel. *J. Heat Transf.* **2011**, *25*, 165–172. [[CrossRef](#)]
80. Kim, S.; Choi, E.Y.; Kwak, J.S. Effect of Channel Orientation on the Heat Transfer Coefficient in the Smooth and Dimpled Rotating Rectangular Channels. *ASME J. Heat Transf.* **2012**, *134*, 064504. [[CrossRef](#)]
81. Chang, S.W.; Liou, T.-M.; Chen, W.-C. Influence of Radial Rotation on Heat Transfer in a Rectangular Channel with Two Opposite Walls Roughened by Hemispherical Protrusions at High Rotation Numbers. *ASME J. Turbomach.* **2011**, *134*, 011010. [[CrossRef](#)]
82. Chang, S.; Liou, T.-M.; Lee, T.-H. Thermal performance comparison between radially rotating ribbed parallelogram channels with and without dimples. *Int. J. Heat Mass Transf.* **2012**, *55*, 3541–3559. [[CrossRef](#)]
83. Chyu, M.K.; Hsing, Y.C.; Shih, T.I.-P.; Natarajan, V. Heat Transfer Contributions of Pins and Endwall in Pin-Fin Arrays: Effects of Thermal Boundary Condition Modeling. *ASME J. Turbomach.* **1999**, *121*, 257–263. [[CrossRef](#)]
84. Chyu, M.K.; Siw, S.C.; Moon, H.K. Effects of Height-to-Diameter Ratio of Pin Element on Heat Transfer from Staggered Pin-Fin Arrays. In Proceedings of the ASME Turbo Expo 2009: Power for Land, Sea, and Air. Volume 3: Heat Transfer, Parts A and B, Orlando, FL, USA, 8–12 June 2009; pp. 705–713. [[CrossRef](#)]
85. Chyu, M.K.; Yen, C.H.; Siw, S.C. Comparison of Heat Transfer from Staggered Pin Fin Arrays with Circular, Cubic and Diamond Shaped Elements. In Proceedings of the ASME Turbo Expo 2007: Power for Land, Sea, and Air. Volume 4: Turbo Expo 2007, Parts A and B, Montreal, QC, Canada, 14–17 May 2007; pp. 991–999. [[CrossRef](#)]
86. Siw, S.C.; Chyu, M.K.; Alvin, M.A. Heat Transfer Enhancement of Internal Cooling Passage with Triangular and Semi-Circular Shaped Pin-Fin Arrays. In Proceedings of the ASME Turbo Expo 2012: Turbine Technical Conference and Exposition. Volume 4: Heat Transfer, Parts A and B, Copenhagen, Denmark, 11–15 June 2012; pp. 493–503. [[CrossRef](#)]
87. Chang, S.W.; Liou, T.-M.; Lee, T.-H. Heat Transfer of a Rotating Rectangular Channel with a Diamond-Shaped Pin-Fin Array at High Rotation Numbers. *ASME J. Turbomach.* **2013**, *135*, 041007. [[CrossRef](#)]
88. Chang, S.W.; Hu, Y.-W. Endwall thermal performances of radially rotating rectangular channel with pin-fins on skewed rib lands. *Int. J. Heat Mass Transf.* **2014**, *69*, 173–190. [[CrossRef](#)]
89. Ullal, A.; Hung, S.-C.; Huang, S.-C.; Liu, Y.-H. Experimental investigation of the effect of compound protrusion-pin array on heat transfer in an internal rotating cooling channel. *Appl. Eng.* **2018**, *140*, 23–33. [[CrossRef](#)]

90. Hung, S.-C.; Huang, S.-C.; Liu, Y.-H. Effect of nonuniform pin size on heat transfer in a rotating rectangular channel with pin-fin arrays. *Appl. Eng.* **2019**, *163*, 114393. [[CrossRef](#)]
91. Saha, K.; Guo, S.; Acharya, S.; Nakamata, C. Heat transfer and pressure measurements in a lattice-cooled trailing edge of a turbine airfoil. In *Turbo Expo: Power for Land, Sea, and Air*; ASME: New York, NY, USA, 2008; Volume 43147, pp. 1117–1125.
92. Pagnacco, F.; Furlani, L.; Armellini, A.; Casarsa, L.; Davis, A. Rotating Heat Transfer Measurements on a Multi-Pass Internal Cooling Channel: II—Experimental Tests. In Proceedings of the ASME Turbo Expo 2016: Turbomachinery Technical Conference and Exposition. Volume 5B: Heat Transfer, Seoul, Korea, 13–17 June 2016; p. V05BT16A004. [[CrossRef](#)]
93. Ledezma, G.A.; Bunker, R.S. The Optimal Distribution of Pin Fins for Blade Tip Cap Underside Cooling. *ASME J. Turbomach.* **2014**, *137*, 011002. [[CrossRef](#)]
94. Sunden, B.; Xie, G. Gas Turbine Blade Tip Heat Transfer and Cooling: A Literature Survey. *Heat Transf. Eng.* **2010**, *31*, 527–554. [[CrossRef](#)]
95. Suryanarayanan, A.; Mhetras, S.P.; Schobeiri, M.T.; Han, J.C. Film-Cooling Effectiveness on a Rotating Blade Platform. *ASME J. Turbomach.* **2008**, *131*, 011014. [[CrossRef](#)]
96. Tamunobere, O.; Acharya, S. Turbine Blade Tip Film Cooling with Blade Rotation—Part I: Tip and Pressure Side Coolant Injection. *ASME J. Turbomach.* **2016**, *138*, 091002. [[CrossRef](#)]
97. Tamunobere, O.; Acharya, S. Turbine Blade Tip Cooling with Blade Rotation—Part II: Shroud Coolant Injection. *ASME J. Turbomach.* **2016**, *138*, 091003. [[CrossRef](#)]
98. Vedula, R.J.; Metzger, D.E. A Method for the Simultaneous Determination of Local Effectiveness and Heat Transfer Distributions in Three-Temperature Convection Situations. In Proceedings of the 36th ASME, International Gas Turbine and Aeroengine Congress and Exposition, Orlando, FL, USA, 3–6 June 1991. Available online: <https://ui.adsabs.harvard.edu/abs/1991gatu.confR...V/exportcitation> (accessed on 18 December 2020).
99. Ekkad, S.V.; Ou, S.; Rivir, R.B. A Transient Infrared Thermography Method for Simultaneous Film Cooling Effectiveness and Heat Transfer Coefficient Measurements from a Single Test. *J. Turbomach.* **2004**, *126*, 597–603. [[CrossRef](#)]
100. Owen, J.M. Flow and Heat Transfer in Rotating-Disc Systems. In *International Symposium on Heat Transfer in Turbomachinery*; Begel House Inc.: New York, NY, USA, 1992; pp. 173–195.
101. Wilson, M.; Pilbrow, R.; Owen, J.M. Flow and Heat Transfer in a Pre-Swirl Rotor-Stator System. In Proceedings of the ASME 1995 International Gas Turbine and Aeroengine Congress and Exposition, Houston, TX, USA, 5–8 June 1995; Volume 3, pp. 364–373. [[CrossRef](#)]
102. Mirzamoghadam, A.V.; Xiao, Z. Flow and Heat Transfer in an Industrial Rotor-Stator Rim Sealing Cavity. *J. Eng. Gas. Turbines Power* **2000**, *124*, 125–132. [[CrossRef](#)]
103. Serre, E.; Bontoux, P.; Launder, B.E. Transitional-turbulent flow with heat transfer in a closed rotor-stator cavity. *J. Turbul.* **2004**, *5*, 1–3. [[CrossRef](#)]
104. Javiya, U.; Chew, J.; Hills, N.J.; Zhou, L.; Wilson, M.; Lock, G.D. CFD Analysis of Flow and Heat Transfer in a Direct Transfer Preswirl System. *ASME J. Turbomach.* **2012**, *134*, 031017. [[CrossRef](#)]
105. Iacovides, H.; Chew, J. The computation of convective heat transfer in rotating cavities. *Int. J. Heat Fluid Flow* **1993**, *14*, 146–154. [[CrossRef](#)]
106. Chew, J.W.; Rolls-Royce plc. Prediction of rotating disc flow and heat transfer in gas turbine engines. In *Rotating Machinery: Proceedings of The International Symposia on Transport Phenomena and Dynamics of Rotating Machinery*; CRC Press: London, UK, 1992; Volume 1, p. 145.
107. Bohn, D.E.; Deutsch, G.N.; Simon, B.; Burkhardt, C. Flow Visualisation in a Rotating Cavity with Axial Throughflow. In Proceedings of the ASME Turbo Expo 2000: Power for Land, Sea, and Air. Volume 3: Heat Transfer; Electric Power; Industrial and Cogeneration, Munich, Germany, 8–11 May 2000; p. V003T01A084. [[CrossRef](#)]
108. Roy, R.P.; Feng, J.; Narzary, D.; Paolillo, R.E. Experiment on Gas Ingestion through Axial-Flow Turbine Rim Seals. *J. Eng. Gas. Turbines Power* **2005**, *127*, 573–582. [[CrossRef](#)]
109. Johnson, B.V.; Wang, C.-Z.; Roy, R.P. A Rim Seal Orifice Model with 2 Cds and Effects of Swirl in Seals. In Proceedings of the ASME Turbo Expo 2008: Power for Land, Sea, and Air. Volume 4: Heat Transfer, Parts A and B, Berlin, Germany, 9–13 June 2008; pp. 1531–1541. [[CrossRef](#)]
110. Balasubramanian, J.; Pathak, P.S.; Thiagarajan, J.K.; Singh, P.N.; Roy, R.P.; Mirzamoghadam, A.V. Experimental Study of Ingestion in the Rotor–Stator Disk Cavity of a Subscale Axial Turbine Stage. *J. Turbomach.* **2015**, *137*, 091010. [[CrossRef](#)]
111. Balasubramanian, J.; Michael, M.; Roy, R.P.; Kim, Y.W.; Moon, H.K. Experiments on Front- and Aft- Disk Cavity Ingestion in a Subscale 1.5-Stage Axial Turbine. In Proceedings of the ASME Turbo Expo 2016: Turbomachinery Technical Conference and Exposition. Volume 5A: Heat Transfer, Seoul, Korea, 13–17 June 2016; p. V05AT15A002. [[CrossRef](#)]
112. Owen, J.M. Prediction of Ingestion Through Turbine Rim Seals—Part I: Rotationally Induced Ingress. *ASME J. Turbomach.* **2010**, *133*, 031005. [[CrossRef](#)]
113. Owen, J.M. Prediction of Ingestion through Turbine Rim Seals—Part II: Externally Induced and Combined Ingress. *ASME J. Turbomach.* **2010**, *133*, 031006. [[CrossRef](#)]
114. Newton, P.J.; Yan, Y.; Stevens, N.E.; Evatt, S.T.; Lock, G.D.; Owen, J.M. Transient heat transfer measurements using thermochromic liquid crystal. Part 1: An improved technique. *Int. J. Heat Fluid Flow* **2003**, *24*, 14–22. [[CrossRef](#)]

-
115. Kakade, V.U.; Lock, G.D.; Wilson, M.; Owen, J.M.; Mayhew, J.E. Accurate heat transfer measurements using thermochromic liquid crystal. Part 2: Application to a rotating disc. *Int. J. Heat Fluid Flow* **2009**, *30*, 950–959. [[CrossRef](#)]
 116. Owen, J.M.; Newton, P.J.; Lock, G.D. Transient heat transfer measurements using thermochromic liquid crystal. Part 2: Experimental uncertainties. *Int. J. Heat Fluid Flow* **2003**, *24*, 23–28. [[CrossRef](#)]
 117. Pountney, O.J.; Sangan, C.M.; Lock, G.D.; Owen, J.M. Effect of Ingestion on Temperature of Turbine Disks. *J. Turbomach.* **2013**, *135*, 051010. [[CrossRef](#)]